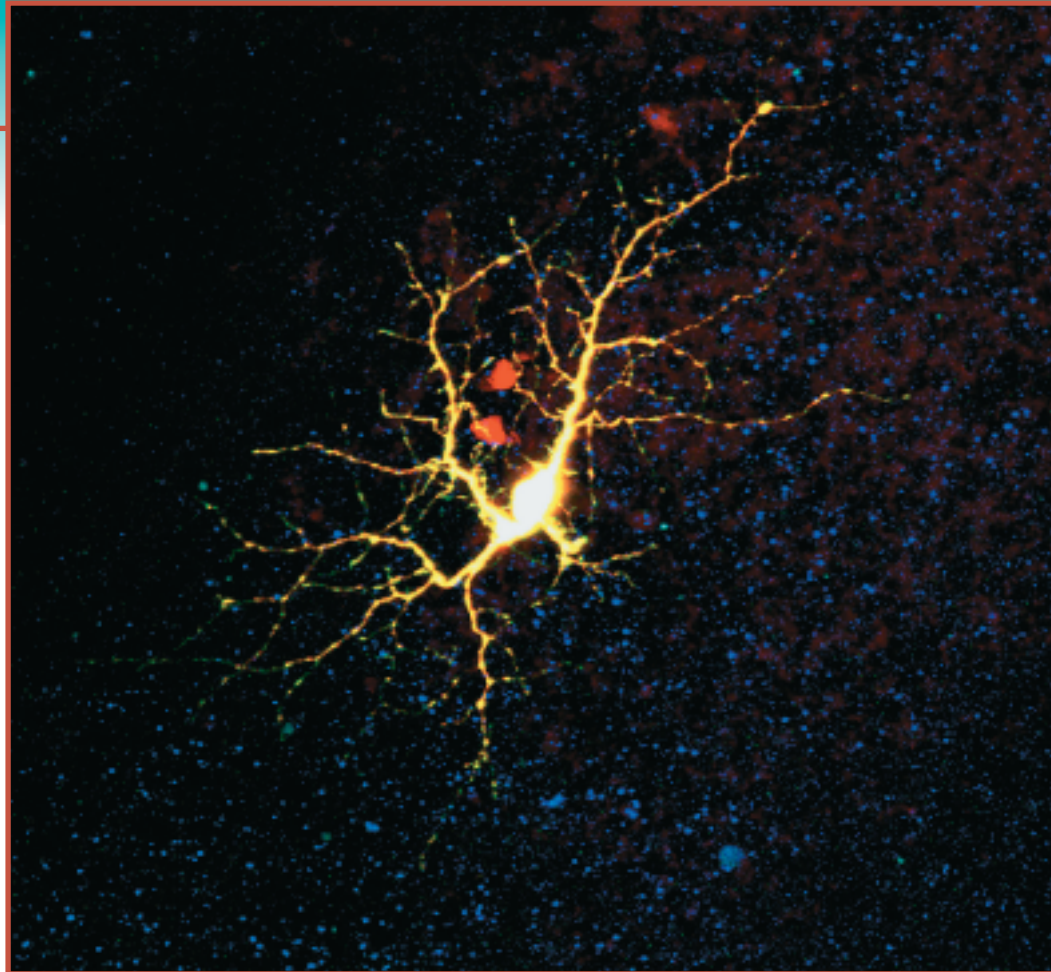# CHAPTER

# 10

*The impermeable membranes of cells, including those of neurons such as that pictured here, permit the establishment of a membrane potential, which changes when certain membrane proteins allow ions to flow into or out of the cell. Different membrane proteins mediate the transmembrane movements of other substances either with or against their concentration gradients. [David Becker/Photo Researchers.]*

# Membrane Transport

Cells are separated from their environments by plasma membranes. Eukaryotic cells, in addition, are compartmentalized by intracellular membranes that form the boundaries and internal structures of their various organelles. Biological membranes present formidable barriers to the passage of ionic and polar substances so that *these substances can traverse membranes only through the action of specific* **transport proteins.** Such proteins are therefore required to mediate all transmembrane movements of ions, such as $Na^+$, $K^+$, $Ca^{2+}$, and $Cl^-$, as well as metabolites such as pyruvate, amino acids, sugars, and nucleotides, and even water. Transport proteins are also responsible for all biological electrochemical phenomena such as neurotransmission. More complicated processes (e.g., endocytosis) are required to move larger substances such as proteins and macromolecular aggregates across membranes.

We begin our discussion of membrane transport by considering the thermodynamics of this process. We will then examine the structures and mechanisms of several different types of transport systems.

## 1  Thermodynamics of Transport

The diffusion of a substance between two sides of a membrane

$$A(out) \rightleftharpoons A(in)$$
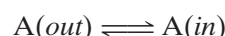
thermodynamically resembles a chemical equilibrium. We saw in Section 1-4D that the free energy of a solute, A, varies with its concentration:

$$\overline{G}_A - \overline{G}_A^{\circ\prime} = RT \ln[A] \qquad [10\text{-}1]$$

where $\overline{G}_A$ is the **chemical potential** (partial molar free energy) of A (the bar indicates quantity per mole) and $\overline{G}_A^{\circ\prime}$ is the chemical potential of its standard state. Thus, a difference in the concentrations of the substance on two sides of a membrane generates a **chemical potential difference:**

$$\Delta\overline{G}_A = \overline{G}_A(in) - \overline{G}_A(out) = RT \ln\left(\frac{[A]_{in}}{[A]_{out}}\right) \qquad [10\text{-}2]$$

Consequently, if the concentration of A outside the membrane is greater than that inside, $\Delta\overline{G}_A$ for the transfer of A from outside to inside will be negative and the spontaneous net flow of A will be inward. If, however, [A] is greater inside than outside, $\Delta\overline{G}_A$ is positive and an inward net flow of A can occur only if an exergonic process, such as ATP hydrolysis, is coupled to it to make the overall free energy change negative (see Sample Calculation 10-1).

The transmembrane movement of ions also results in charge differences across the membrane, thereby generating an electrical potential difference, $\Delta\Psi = \Psi(in) - \Psi(out)$, where $\Delta\Psi$ is termed the **membrane potential.** Consequently, if A is ionic, Eq. 10-2 must be amended to include the electrical work required to transfer a mole of A across the membrane from outside to inside:

$$\Delta\overline{G}_A = RT \ln\left(\frac{[A]_{in}}{[A]_{out}}\right) + Z_A\mathscr{F}\Delta\Psi \qquad [10\text{-}3]$$

where $Z_A$ is the ionic charge of A; $\mathscr{F}$, the Faraday constant, is the charge of a mole of electrons ($96,485 \text{ C}\cdot\text{mol}^{-1}$; C is the symbol for coulomb); and $\overline{G}_A$ is now termed the **electrochemical potential** of A. The membrane potentials of living cells are commonly as high as $-100 \text{ mV}$ (inside negative;

### SAMPLE CALCULATION 10-1

Show that $\Delta G < 0$ when $Ca^{2+}$ ions move from the endoplasmic reticulum (where $[Ca^{2+}] = 1 \text{ mM}$) to the cytosol (where $[Ca^{2+}] = 0.1 \text{ μM}$). Assume $\Delta\Psi = 0$.

The cytosol is *in* and the endoplasmic reticulum is *out*.

$$\Delta G = RT\ln\frac{[Ca^{2+}]_{in}}{[Ca^{2+}]_{out}} = RT \ln\frac{10^{-7}}{10^{-3}}$$
$$= RT(-9.2)$$

Hence, $\Delta G$ is negative.

note that $1 \text{ V} = 1 \text{ J} \cdot \text{C}^{-1}$). Hence, the last term in Eq. 10-3 is often significant for ionic substances, particularly in mitochondria (Chapter 17) and in neurotransmission (Section 10-2C).

**Transport May Be Mediated or Nonmediated.** There are two types of transport processes: **nonmediated transport** and **mediated transport.** Nonmediated transport occurs through simple diffusion. In contrast, mediated transport occurs through the action of specific carrier proteins. The driving force for the nonmediated flow of a substance through a medium is its chemical potential gradient. Thus, *the substance diffuses in the direction that eliminates its concentration gradient, at a rate proportional to the magnitude of this gradient. The rate of diffusion of a substance also depends on its solubility in the membrane's nonpolar core*. Consequently, nonpolar molecules such as steroids and $O_2$ readily diffuse through biological membranes by nonmediated transport, according to their concentration gradients across the membranes.

Mediated transport is classified into two categories depending on the thermodynamics of the system:

1. **Passive-mediated transport,** or **facilitated diffusion,** in which a specific molecule flows from high concentration to low concentration.

2. **Active transport,** in which a specific molecule is transported from low concentration to high concentration, that is, against its concentration gradient. Such an endergonic process must be coupled to a sufficiently exergonic process to make it favorable (i.e., $\Delta G < 0$).

## 2 Passive-Mediated Transport

Substances that are too large or too polar to diffuse across lipid bilayers on their own may be conveyed across membranes via proteins or other molecules that are variously called **carriers, permeases, channels,** and **transporters.** These transporters operate under the same thermodynamic principles but vary widely in structure and mechanism, particularly as it relates to their selectivity.

### A Ionophores

Ionophores are organic molecules of diverse types, often of bacterial origin, that increase the permeability of membranes to ions. These molecules often exert an antibiotic effect by discharging the vital ion concentration gradients that cells actively maintain.

There are two types of ionophores:

1. *Carrier ionophores,* which increase the permeabilities of membranes to their selected ion by binding it, diffusing through the membrane, and releasing the ion on the other side (Fig. 10-1a). For net transport to occur, the uncomplexed ionophore must then return to the original side of the membrane ready to repeat the process. Carriers therefore share the common property that *their ionic complexes are soluble in nonpolar solvents.*

2. *Channel forming ionophores,* which form transmembrane channels or pores through which their selected ions can diffuse (Fig. 10-1b).

Both types of ionophores transport ions at a remarkable rate. For example, a single molecule of the carrier ionophore **valinomycin** transports up
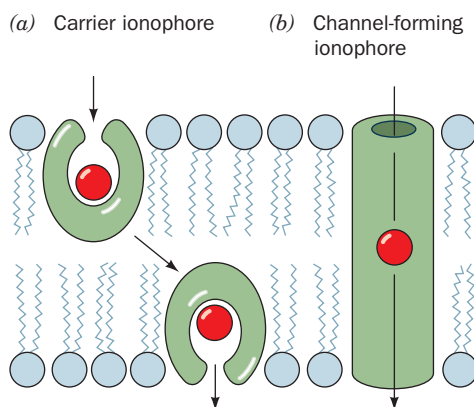


*(a)* Carrier ionophore  *(b)* Channel-forming ionophore

**Figure 10-1 Ionophore action.** (*a*) Carrier ionophores transport ions by diffusing through the lipid bilayer. (*b*) Channel-forming ionophores span the membrane with a channel through which ions can diffuse.
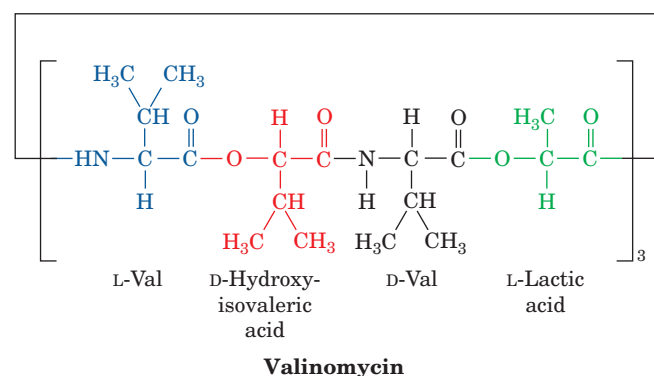
**Figure 10-2   Valinomycin.**   This cyclic ionophore contains ester and amide bonds and D- as well as L-amino acids.

to $10^4$ K$^+$ ions per second across a membrane. Channel formers have an even greater ion throughput; for example, each membrane channel composed of the antibiotic **gramicidin A** permits the passage of over $10^7$ K$^+$ ions per second. Clearly, the presence of either type of ionophore, even in small amounts, greatly increases the permeability of a membrane toward the specific ions transported. However, *since ionophores passively permit ions to diffuse across a membrane in either direction, their effect can only be to equilibrate the concentrations of their selected ions across the membrane.*

Valinomycin, which is one of the best characterized ionophores, specifically binds K$^+$. It is a cyclic molecule containing D- and L-amino acid residues that participate in ester linkages as well as peptide bonds (Fig. 10-2). The X-ray structure of valinomycin's K$^+$ complex (Fig. 10-3) indicates that the K$^+$ ion is octahedrally coordinated by the carbonyl groups of its six Val residues, and the cyclic valinomycin backbone surrounds the K$^+$ coordination shell. The methyl and isopropyl side chains project outward to provide the complex with a nonpolar exterior that makes it soluble in the hydrophobic cores of lipid bilayers.

The K$^+$ ion (ionic radius, $r = 1.33$ Å) fits snugly into valinomycin's coordination site, but the site is too large for Na$^+$ ($r = 0.95$ Å) or Li$^+$ ($r = 0.60$ Å) to coordinate with all six carbonyl oxygens. Valinomycin therefore has 10,000-fold greater binding affinity for K$^+$ than for Na$^+$. No other known substance discriminates better between Na$^+$ and K$^+$.

Gramicidin A is a 15-residue linear polypeptide consisting of alternating L and D residues, all of which are hydrophobic (Fig. 10-4). NMR and
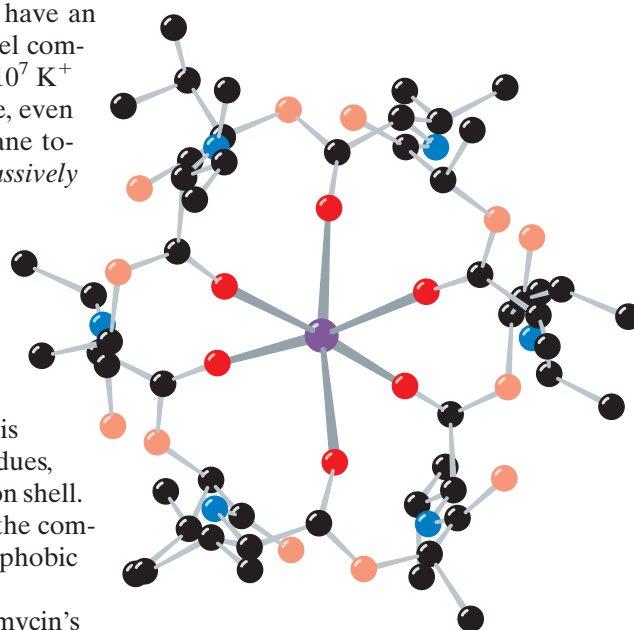


**Figure 10-3   X-Ray structure of valinomycin in complex with a K$^+$ ion.**   Six oxygen atoms (*dark red*) octahedrally coordinate the K$^+$ ion (*purple*). [After Neupert-Laves, K. and Dobler, M., *Helv. Chim. Acta* **58,** 439 (1975).]



**Gramicidin A**

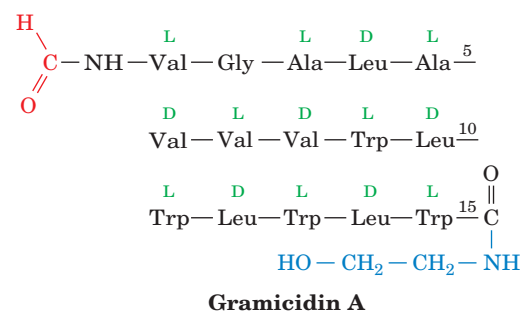**Figure 10-4   Gramicidin A.**   This 15-residue peptide of alternating D- and L-amino acids is chemically blocked at both its N- and C-termini.
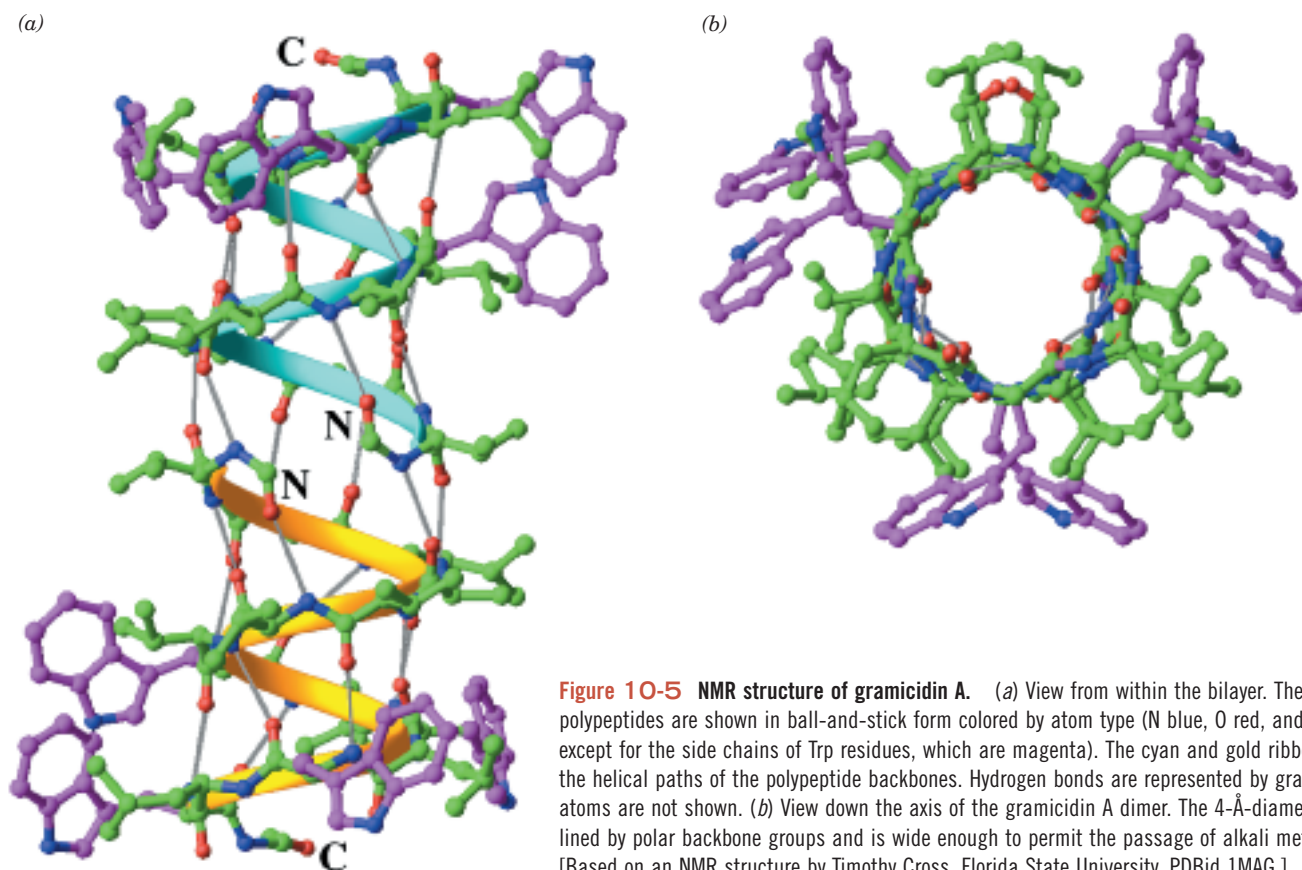
(a)



(b)



**Figure 10-5  NMR structure of gramicidin A.**   (a) View from within the bilayer. The two polypeptides are shown in ball-and-stick form colored by atom type (N blue, O red, and C green except for the side chains of Trp residues, which are magenta). The cyan and gold ribbons indicate the helical paths of the polypeptide backbones. Hydrogen bonds are represented by gray lines. H atoms are not shown. (b) View down the axis of the gramicidin A dimer. The 4-Å-diameter channel is lined by polar backbone groups and is wide enough to permit the passage of alkali metal cations. [Based on an NMR structure by Timothy Cross, Florida State University. PDBid 1MAG.]

X-ray crystallographic evidence indicates that gramicidin A dimerizes in a head-to-head fashion to form a transmembrane channel (Fig. 10-5). The alternating L and D residues of gramicidin A allow it to form a helix with a nonpolar exterior and a polar central channel that facilitates the passage of $Na^+$ and $K^+$ ions. Recall that a standard α helix contains only L amino acids and does not have a hollow core (Section 6-1B).

## B  Porins

The porins, introduced in Section 9-3A, are β barrel structures with a central aqueous channel. In the *E. coli* OmpF porin (Fig. 9-24), the channel is constricted to form an elliptical pore with a minimum cross section of $7 \times 11$ Å. Consequently, solutes of more than ~600 D are too large to pass through the channel. OmpF is weakly cation selective; other porins are more selective for anions. In general, the size of the channel and the residues that form its walls determine what types of substances can pass through.

Solute selectivity is elegantly illustrated by **maltoporin.** This bacterial outer membrane protein facilitates the diffusion of **maltodextrins,** which are the α(1→4)-linked glucose oligosaccharide degradation products of starch (for example, the glucose disaccharide maltose). The X-ray structure of *E. coli* maltoporin reveals that the protein is structurally similar to OmpF porin but is a homotrimer of 18-stranded rather than 16-stranded antiparallel β barrels. Three long loops from the extracellular face of each maltoporin subunit fold inward into the barrel, thereby constricting the channel near the center of the membrane to a diameter of ~5 Å and giving the channel an hourglass-like cross section. The channel is lined on one side

with a series of six contiguous aromatic side chains arranged in a left-handed helical path that matches the left-hand helical curvature of α-amylose (Fig. 8-10). This so-called greasy slide extends from one end of the channel, through its constriction, to the other end (Fig. 10-6).

How does the greasy slide work? The hydrophobic faces of the maltodextrin glucose residues stack on aromatic side chains, as is often observed in complexes of sugars with proteins. The glucose hydroxyl groups, which are arranged in two strips along opposite edges of the maltodextrins, form numerous hydrogen bonds with polar and charged side chains that line the channel. Tyr 118, which protrudes into the channel opposite the greasy slide, apparently functions as a steric barrier that only permits the passage of near-planar groups such as glucosyl residues. Thus, the hook-shaped sucrose (a glucose–fructose disaccharide) passes only very slowly through the maltoporin channel.

At the start of the translocation process, the entering glucosyl residue interacts with the readily accessible end of the greasy slide in the extracellular vestibule of the channel. Further translocation along the helical channel requires the maltodextrin to follow a screwlike path that maintains the helical structure of the oligosaccharide, much like the movement of a bolt through a nut, thereby excluding molecules of comparable size that have different shapes. *The translocation process is unlikely to encounter any large energy barrier due to the smooth surface of the greasy slide and the multiple polar groups at the channel constriction that would permit the essentially continuous exchange of hydrogen bonds as a maltodextrin moves through the constriction.*

## C   Ion Channels

All cells contain ion-specific channels that allow the rapid passage of ions such as $Na^+$, $K^+$, and $Cl^-$. The movement of these ions through such channels, along with their movement through active transporters (discussed in Section 10-3), is essential for maintaining osmotic balance, for signal transduction (Section 21-3), and for effecting changes in membrane potential that are responsible for neurotransmission. Mammalian cells, for example, maintain a nonequilibrium distribution of ions on either side of the plasma membrane: ~150 mM $Na^+$ and ~4 mM $K^+$ in the extracellular fluid, and ~12 mM $Na^+$ and ~140 mM $K^+$ inside the cell.

Potassium ions passively diffuse from the cytoplasm to the extracellular space through transmembrane proteins known as **$K^+$ channels.** Although there is a large diversity of $K^+$ channels, even within a single organism, all of them have similar sequences, exhibit comparable permeability characteristics, and most importantly, are at least 10,000-fold more permeable to $K^+$ than $Na^+$. Since this high selectivity (around the same as that of valinomycin; Section 10-2A) implies energetically strong interactions between $K^+$ and the protein, how can the $K^+$ channel maintain its observed nearly diffusion-limited throughput rate of up to $10^8$ ions per second (a $10^4$-fold greater rate than that of valinomycin)?

**The X-Ray Structure of KcsA Reveals the Basis of $K^+$ Channel Selectivity.**   One of the best characterized ion channels is a $K^+$ channel from *Streptomyces lividans* named **KcsA.** This 158-residue integral membrane protein, like all known $K^+$ channels, functions as a homotetramer. As we shall see, the KcsA channel's three-dimensional structure explains both its functional features and serves as a model for more complicated eukaryotic $K^+$ channels.

The X-ray structure of KcsA's N-terminal 125-residue segment, determined by Roderick MacKinnon, reveals that each of its subunits forms
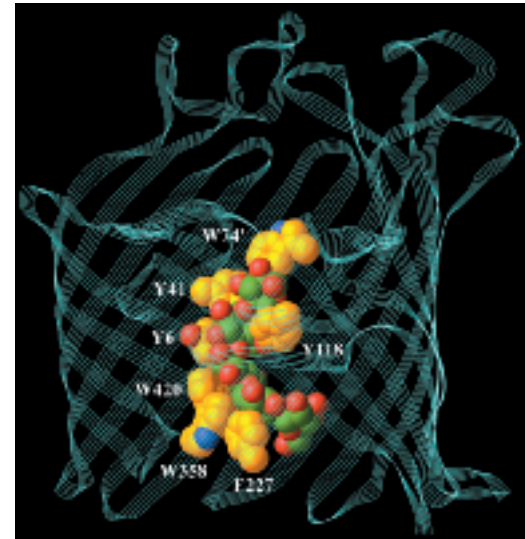


**Figure 10-6   Structure of a maltoporin subunit in complex with a maltodextrin of six glycosyl units.**   The polypeptide backbone of this *E. coli* protein is represented by a cyan ribbon. Five glucose residues of maltodextrin and the aromatic side chains lining the transport channel are shown in space-filling form with N blue, O red, protein C gold, and glucosyl C green. The "greasy slide" consists of the aromatic side chains of six residues. Tyr 118, which projects into the channel, helps restrict passage to glucosyl residues. [Based on an X-ray structure by Tilman Schirmer, University of Basel, Basel, Switzerland. PDBid 1MPO.]
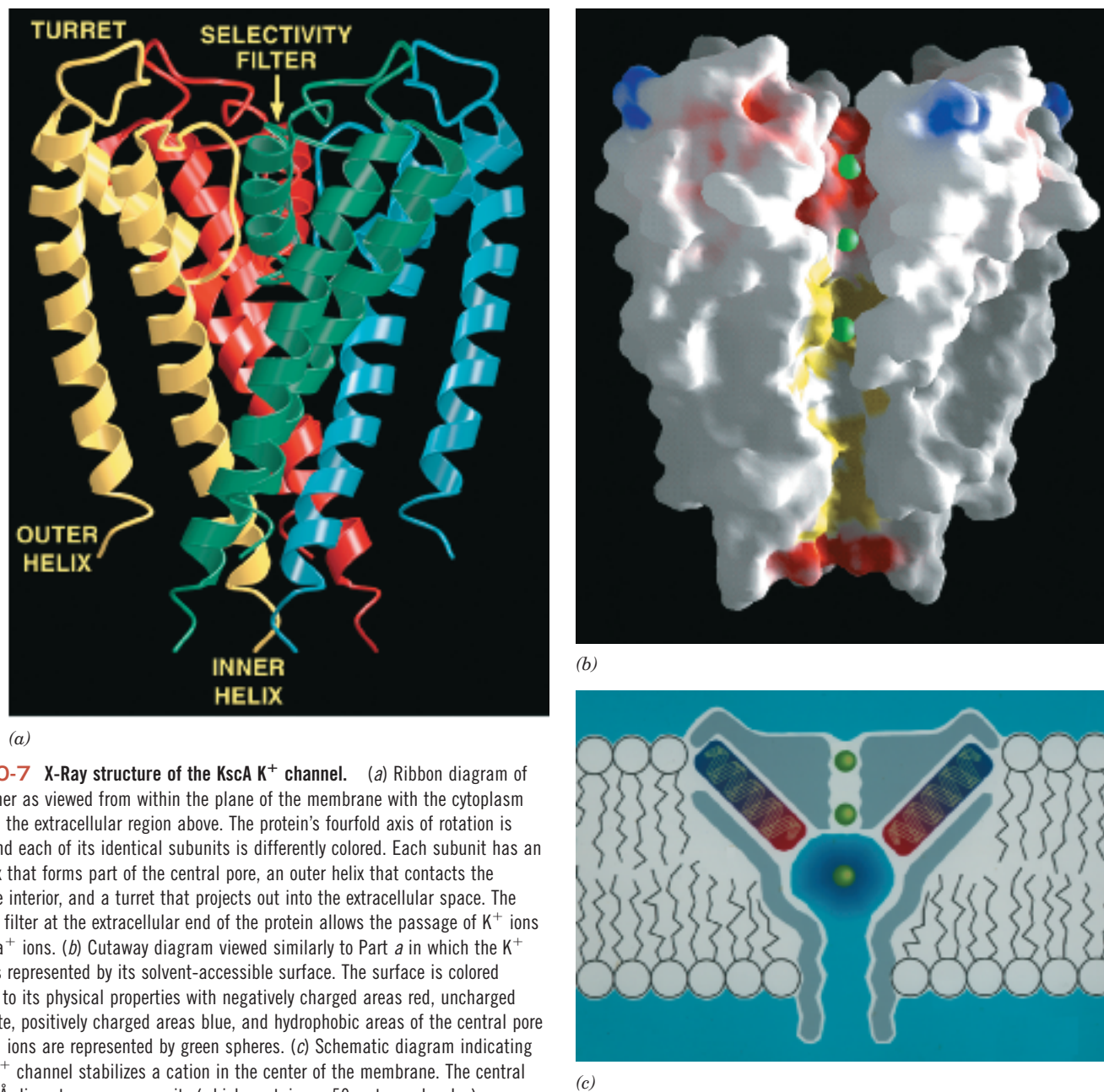
(a)



(b)

**Figure 10-7    X-Ray structure of the KscA K⁺ channel.**    (*a*) Ribbon diagram of the tetramer as viewed from within the plane of the membrane with the cytoplasm below and the extracellular region above. The protein's fourfold axis of rotation is vertical and each of its identical subunits is differently colored. Each subunit has an inner helix that forms part of the central pore, an outer helix that contacts the membrane interior, and a turret that projects out into the extracellular space. The selectivity filter at the extracellular end of the protein allows the passage of $K^+$ ions but not $Na^+$ ions. (*b*) Cutaway diagram viewed similarly to Part *a* in which the $K^+$ channel is represented by its solvent-accessible surface. The surface is colored according to its physical properties with negatively charged areas red, uncharged areas white, positively charged areas blue, and hydrophobic areas of the central pore yellow. $K^+$ ions are represented by green spheres. (*c*) Schematic diagram indicating how the $K^+$ channel stabilizes a cation in the center of the membrane. The central pore's 10-Å-diameter aqueous cavity (which contains ~50 water molecules) stabilizes a $K^+$ ion (*green sphere*) in the otherwise hydrophobic membrane interior. In addition, the C-terminal ends of the pore helices (*red*) all point toward the $K^+$ ion, thereby electrostatically stabilizing it via their dipole moments (the alignment of their polar group dipoles makes α helices negative at their C-terminal ends). [Courtesy of Roderick MacKinnon, Rockefeller University. PDBid 1BL8.]



(c)

two nearly parallel transmembrane helices that are connected by an ~20-residue pore region (Fig. 10-7*a*). Four such subunits associate to form a fourfold symmetric assembly surrounding a central pore. The four inner (C-terminal) helices, which largely form the pore, pack against each other near the cytoplasmic side of the membrane much like the poles of an inverted teepee. The four outer helices, which face the lipid bilayer, buttress the inner helices. Several $K^+$ ions and ordered water molecules are seen to occupy the central pore (Figs. 10-7*b* and 10-8*a*).
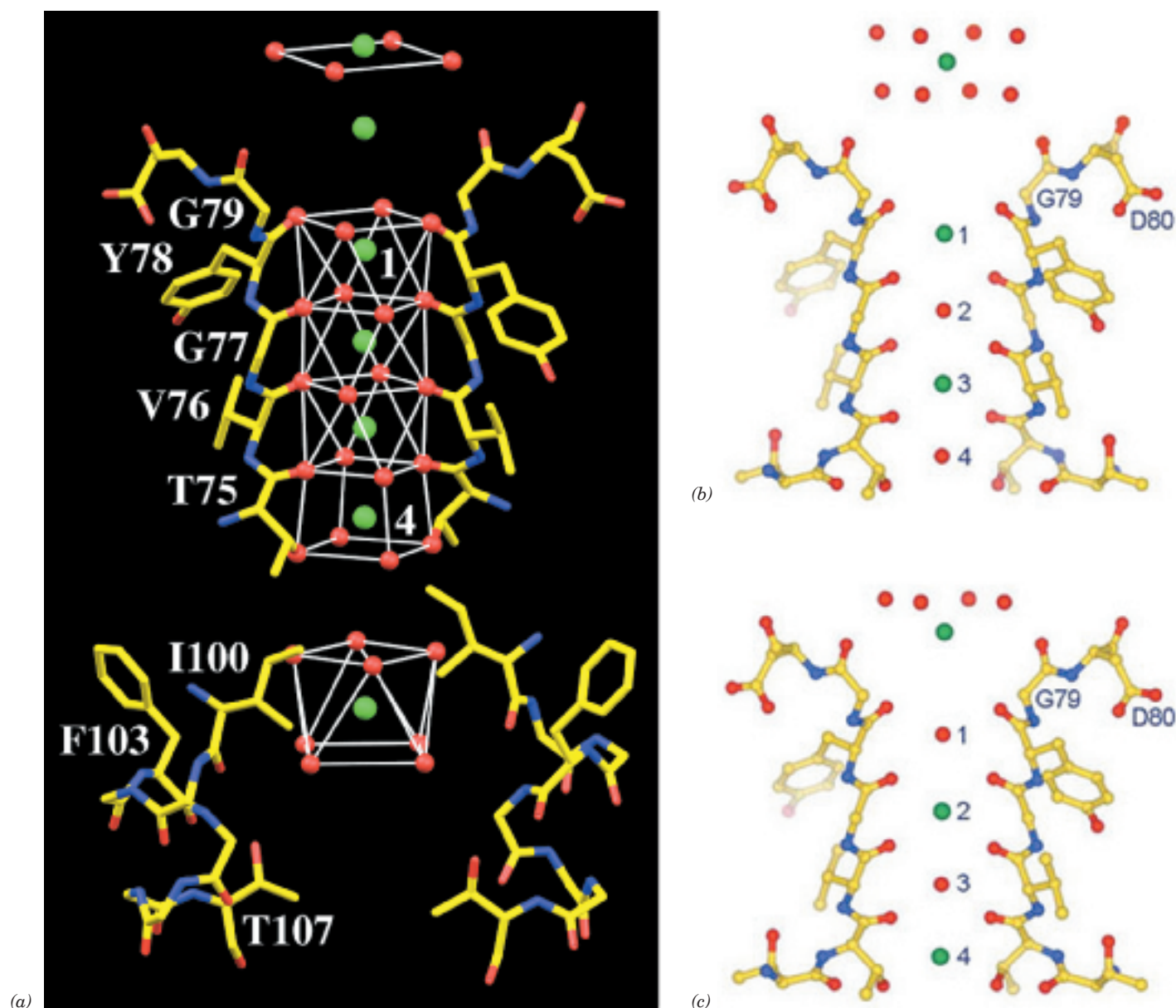
**Figure 10-8  Portions of the KcsA K$^+$ channel responsible for its ion selectivity viewed similarly to Fig. 10-7.** (*a*) The X-ray structure of the residues forming the cavity (*bottom*) and selectivity filter (*top*) but with the front and back subunits omitted for clarity. Atoms are colored according to type with C yellow, N blue, O red, and K$^+$ ions represented by green spheres. The water and protein O atoms that ligand the K$^+$ ions, including those contributed by the front and back subunits, are represented by red spheres. The coordination polyhedra formed by these O atoms are outlined by thin white lines. (*b* & *c*) Two alternative K$^+$ binding states of the selectivity filter, whose superposition is presumed to be responsible for the electron density observed in the X-ray structure of KcsA. Atoms are colored as in Part *a*. Note that K$^+$ ions occupying the selectivity filter are interspersed with water molecules and that the K$^+$ ion immediately above the selectivity filter in Part *b* is further above the protein than that in Part *c*. Hence these ions maintain a constant spacing while traversing the selectivity filter. [Part *a* based on an X-ray structure by, and Parts *b* and *c* courtesy of, Roderick MacKinnon, Rockefeller University. PDBid 1K4C.]  ✷ **See the Interactive Exercises.**

The 45-Å-long central pore has variable width: It starts at its cytoplasmic side (Fig. 10-7*b, bottom*) as an ~6-Å-diameter and 18-Å-long tunnel, the so-called internal pore, whose entrance is lined with four anionic side chains (red area at the bottom of Fig. 10-7*b*) that presumably attract cations and repel anions. The internal pore then widens to form an ~10-Å-diameter cavity. These regions of the central pore are both wide enough so that a K$^+$

ion could move through them in its hydrated state. However, the upper part of the pore, the so-called selectivity filter, narrows to 3 Å thereby forcing a transiting $K^+$ ion to shed its waters of hydration. The walls of the internal pore and the cavity are lined with hydrophobic groups that interact minimally with diffusing ions (yellow area of the pore in Fig. 10-7b). However, the selectivity filter (red area of the pore at the top of Fig. 10-7b) is lined with closely spaced main chain carbonyl oxygens of residues (Fig. 10-8a, top) that are highly conserved in all $K^+$ channels (their so-called signature sequence, TVGYG) and whose mutations disrupt the ability of the channel to discriminate between $K^+$ and $Na^+$ ions.

What is the function of the cavity? Energy calculations indicate that an ion moving through a narrow transmembrane pore must surmount an energy barrier that is maximal at the center of the membrane. The existence of the cavity reduces this electrostatic destabilization by surrounding the ion with polarizable water molecules (Fig. 10-7c). Remarkably, the $K^+$ ion occupying the cavity is liganded by 8 ordered water molecules located at the corners of a square antiprism (a cube with one face twisted by 45° with respect to the opposite face) in which the $K^+$ ion is centered (Fig. 10-8a, bottom). $K^+$ in aqueous solution is known to have such an inner hydration shell but it had never before been visualized. The $K^+$ ion is precisely centered in the cavity but its liganding water molecules are not in van der Waals contact with the walls of the cavity. Indeed, there is room in the cavity for ~40 additional water molecules although they are unseen in the X-ray structure because they are disordered. This disorder arises because the cavity is lined with hydrophobic groups (mainly the side chains of Ile 100 and Phe 103; Fig. 10-8a) that interact but weakly with water molecules, which are thus free to interact with the $K^+$ ion so as to form an outer hydration shell.

How does the $K^+$ channel discriminate so acutely between $K^+$ and $Na^+$ ions? The main chain O atoms lining the selectivity filter form a stack of rings (Fig. 10-8a; top) that provide a series of closely spaced sites of appropriate dimensions for coordinating dehydrated $K^+$ ions but not the smaller $Na^+$ ions. The structure of the protein surrounding the selectivity filter suggests that the diameter of the pore is rigidly maintained, thus making the energy of a dehydrated $Na^+$ in the selectivity filter considerably higher than that of hydrated $Na^+$ and thereby accounting for the $K^+$ channel's high selectivity for $K^+$ ions.

Since the selectivity filter appears designed to specifically bind $K^+$ ions, how does it support such a high throughput of these ions (up to $10^8$ ions per second)? Figure 10-8a shows what appears to be four $K^+$ ions in the selectivity filter and two more just outside it on its extracellular (top) side. Such closely spaced positive ions would strongly repel one another and hence represent a high energy situation. However, a variety of evidence suggests that this structure is really a superposition of two sets of $K^+$ ions, one with $K^+$ ions at the topmost position in Fig. 10-8a and at positions 1 and 3 in the selectivity filter (Fig. 10-8b) and the second with $K^+$ ions at the second position from the top in Fig. 10-8a and at positions 2 and 4 in the selectivity filter (Fig. 10-8c; X-ray structures can show overlapping atoms because they are averages of many unit cells). Within the selectivity filter, the positions not occupied by $K^+$ ions are instead occupied by water molecules that coordinate the neighboring $K^+$ ions.

The electron density that is represented as the topmost four water molecules in Fig. 10-8a is highly elongated in the vertical direction in this otherwise high resolution (2.0 Å) structure. Hence it is thought to actually arise from eight water molecules that ligand the topmost $K^+$ ion in Fig. 10-8b to form an inner hydration shell similar to that of the $K^+$ in the central cav-

ity (Fig. 10-8*a, bottom*). Moreover, the four water molecules liganding the topmost $K^+$ ion in Fig. 10-8*c* also contribute to this electron density. This latter ring of four waters provides half of the associated $K^+$ ion's eight liganding O atoms. The others are contributed by the carbonyl O atoms of the four Gly 79 residues, which are properly oriented to do so. It therefore appears that a dehydrated $K^+$ ion transits the selectivity filter (moves to successive positions in Fig. 10-8*b,c*) by exchanging the properly spaced ligands extending from its walls, and then exits into the extracellular solution by exchanging protein ligands for water molecules to again acquire a hydration shell. These ligands are spaced and oriented such that there is little free energy change (estimated to be <12 kJ·mol$^{-1}$) as a $K^+$ ion transits the selectivity filter and enters the extracellular solution. The rapid dehydration of the $K^+$ ion entering the selectivity channel from the cavity is, presumably, similarly managed. The essentially level free energy landscape throughout this process is, of course, conducive to the rapid transit of $K^+$ ions through the ion channel and hence must be a product of evolutionary fine-tuning. Energy calculations indicate that mutual electrostatic repulsions between successive $K^+$ ions, whose movements are concerted, balances the attractive interactions holding these ions in the selectivity filter and hence further facilitates their rapid transit.

**Ion Channels Are Gated.**   The physiological functions of ion channels depend not only on their exquisite ion specificity and speed of transport but also on their ability to be selectively opened or closed. For example, the ion gradients across cell membranes, which are generated by specific energy-driven pumps (Section 10-3), are discharged through $Na^+$ and $K^+$ channels. However, the pumps could not keep up with the massive fluxes of ions passing through the open channels, so *ion channels are normally shut and only open transiently to perform some specific task for the cell.* The opening and closing of ion channels, a process known as **gating,** can occur in response to a variety of stimuli:

1. **Mechanosensitive channels** open in response to local deformations in the lipid bilayer. Consequently, they respond to direct physical stimuli such as touch, sound, and changes in osmotic pressure.
2. **Ligand-gated channels** open in response to an extracellular chemical stimulus such as a neurotransmitter.
3. **Signal-gated channels** open on intracellularly binding a $Ca^{2+}$ ion or some other signaling molecule (Section 21-3).
4. **Voltage-gated channels** open in response to a change in membrane potential. Multicellular organisms contain numerous varieties of voltage-gated channels, including those responsible for generating nerve impulses.

**Nerve Impulses Are Propagated by Action Potentials.**   As an example of the functions of voltage-gated channels, let us consider electrical signaling events in neurons (nerve cells). The stimulation of a neuron, a cell specialized for electrical signaling, causes $Na^+$ channels to open so that $Na^+$ ions spontaneously flow into the cell. The consequent local increase in membrane potential induces neighboring voltage-gated $Na^+$ channels to open. The resulting local **depolarization** of the membrane induces nearby voltage-gated $K^+$ channels to open. This allows $K^+$ ions to spontaneously flow out of the cell in a process called **repolarization** (Fig. 10-9). However, well before the distribution of $Na^+$ and $K^+$ ions across the membrane equilibrates, the $Na^+$ and $K^+$ channels spontaneously close. Yet, because depolarization
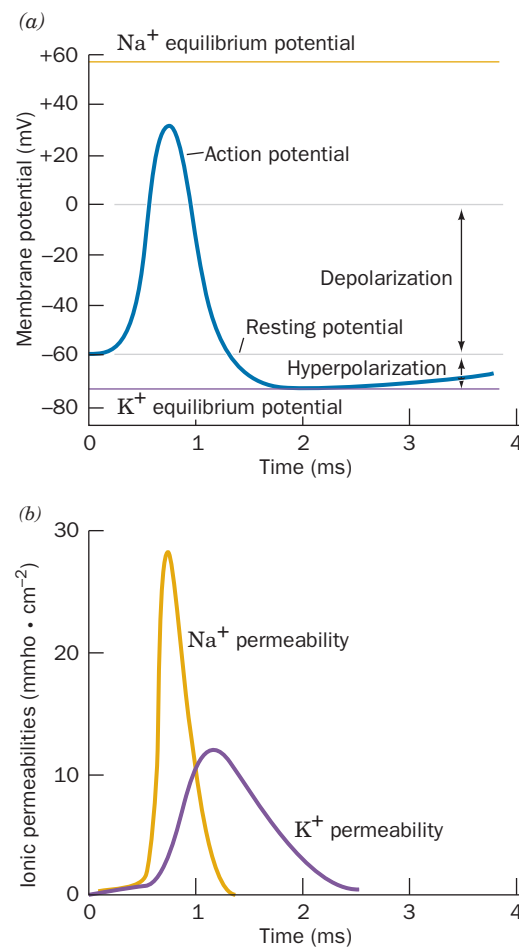


**Figure 10-9** **Time course of an action potential.** (*a*) The axon membrane undergoes rapid depolarization, followed by a nearly as rapid hyperpolarization and then a slow recovery to its resting potential. (*b*) The depolarization is caused by a transient increase in $Na^+$ permeability (conductance), whereas the hyperpolarization results from a more prolonged increase in $K^+$ permeability that begins a fraction of a millisecond later. [After Hodgkin, A.L. and Huxley, A.F., *J. Physiol.* **117,** 530 (1952).]

of a membrane segment induces the voltage-gated $Na^+$ channels in a neighboring membrane segment to open, which induces their neighboring voltage-gated $Na^+$ channels to open, etc., a wave of transient change in the membrane potential, called an **action potential,** travels along the length of the nerve cell (which may be over 1 m long). The action potential, which travels at ~10 m/s, propagates in one direction only because, after the ion channels have spontaneously closed, they resist reopening until the membrane potential has regained its resting value, which takes a few milliseconds (Fig. 10-9).

As an action potential is propagated along the length of a nerve cell, it is continuously renewed so that its signal strength remains constant (in contrast, an electrical impulse traveling down a wire dissipates as a consequence of resistive and capacitive effects). Nevertheless, the relative ion imbalance responsible for the resting membrane potential is small; only a tiny fraction of a nerve cell's $Na^+$–$K^+$ gradient (which is generated by ion pumps; Section 10-3A) is discharged by a single nerve impulse (only one $K^+$ ion per 3000–300,000 in the cytosol is exchanged for extracellular $Na^+$ as indicated by measurements with radioactive $Na^+$). A nerve cell can therefore transmit a nerve impulse every few milliseconds without letup. This capacity to fire rapidly is an essential feature of neuronal communications: Since action potentials all have the same amplitude, the magnitude of a stimulus is conveyed by the rate at which a nerve fires.

**Voltage Gating in $K_V$ Channels Is Triggered by the Motion of Protein Paddles through the Membrane.**   The subunits of all voltage-gated $K^+$ channels contain an ~220-residue N-terminal cytoplasmic domain, an ~250-residue transmembrane domain consisting of six helices, S1 to S6, and an ~150-residue C-terminal cytoplasmic domain (Fig. 10-10). S5 and S6, with their intervening so-called P loop, are homologous to the KcsA channel (Fig. 10-7). In the voltage-gated $K^+$ channels known as **$K_V$ channels,** a conserved ~100-residue loop called the T1 domain precedes the transmembrane domain. In the tetrameric ion channel, the four T1 domains presumably hang from the cytoplasmic face of the $K_V$ channel's transmembrane domain, forming the outer vestibule of the $K^+$ pore.

What is the nature of the gating machinery in voltage-gated ion channels? The ~19-residue S4 helix, which contains approximately five positively charged side chains spaced about every three residues on an otherwise hydrophobic polypeptide, appears to act as a voltage sensor. This was shown by covalently linking a dye, whose fluorescence spectrum varies with the polarity of the environment, to any of several residues in S4. Fluorescence measurements revealed that when the membrane potential increases (the inside becomes less negative), a stretch of at least seven residues at the N-terminal end of S4 moves from a position within the membrane to the extracellular environment. It seems likely that this movement triggers channel opening by displacing a gate that is formed, at least in part, by the cytoplasmic ends of each ion channel's four S6 helices.

Since charged residues are unstable in a lipid environment, it had been widely assumed that the S4 helix remains surrounded by protein throughout its movement. However, this view has been challenged by the X-ray structure, also determined by MacKinnon, of the voltage-dependent $K^+$ channel named **$K_V$AP** from the thermophilic archaebacterium *Aeropyrum pernix*. $K_V$AP is closely similar in sequence and electrophysiological properties to eukaryotic $K_V$ channels. Its S5–P-loop–S6 segment, not surpris-
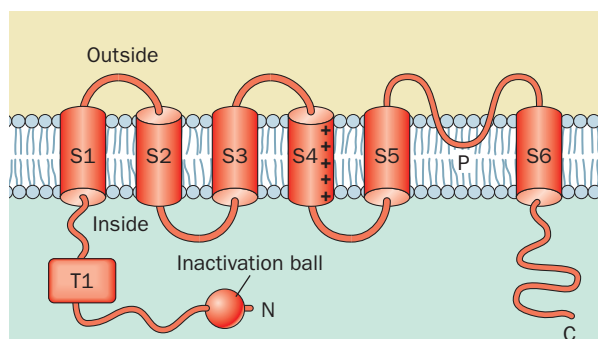


**Figure 10-10  Predicted secondary structure and membrane orientation of voltage-gated $K^+$ channels.** The conserved TVGYG signature sequence is located in the P loop.

**Figure 1O-11  X-Ray structure of the K$_v$AP channel.**    Each of the four subunits is a different color. (*a*) View from the cytoplasmic side of the membrane. The helices of the blue subunit are labeled numerically for S1 to S6 and the pore helix is labeled P. (*b*) View from within the membrane with the cytoplasm below (from the top in Part *a*). Side chains (*green*) of selected residues that participate in voltage-dependent gating are shown for the blue and red subunits. [Courtesy of Roderick MacKinnon, Rockefeller University. PDBid 1ORQ.]

*(a)*

*(b)*

ingly, forms a tetrameric pore structure that is nearly identical to that of KcsA (Fig. 10-7; K$_V$AP's selectivity filter has the signature sequence TVGYG). However, contrary to expectation, helices S3b and S4 form a paddle-shaped assembly that is located on the periphery of the protein such that it extends into the lipid bilayer (Fig. 10-11; the predicted helix S3 is now seen to actually consist of two helices, termed S3a and S3b, joined by a short loop). The paddle has a flexible connection to the rest of the protein as is indicated by comparison to the X-ray structure of segments S1 to S4 alone. This suggests that the K$_V$ channel's four paddles move through the fluid portion of the bilayer toward the cell's exterior in response to an increase in membrane potential (Fig. 10-12) so as to induce a conformational change in the K$^+$ pore that causes it to open. This model is corroborated by experiments that show that the voltage sensor paddles are accessible to tight-binding agents (e.g., antibodies that specifically bind to the loop connecting helices S3b and S4) only from the plasma membrane's cytoplasmic surface when the K$^+$ channel is closed but are only accessible from the membrane's extracellular surface when the channel is open.

   Despite the foregoing, a variety of evidence, such as cross-linking studies, indicate that the S4 helix remains in contact with the pore domain during its voltage-induced movement and thus suggests that the observed conformation of the S3b–S4 paddle is an artifact of K$_V$AP crystallization. It is just such discrepancies that spur further research leading to a better understanding of the phenomenon in question.

**Ion Channels Have Two Gates.**    Electrophysiological measurements indicate that K$_V$ channels spontaneously close a few milliseconds after opening and do not reopen until after the membrane has regained its resting membrane potential. Evidently, *the K$_V$ channel contains two voltage-sensitive gates, one to open the channel on an increase in membrane potential and one to close it a short time later*. This **inactivation** (closing) of the K$_V$ channel is abolished by proteolytically excising its N-terminal 20-residue segment, which
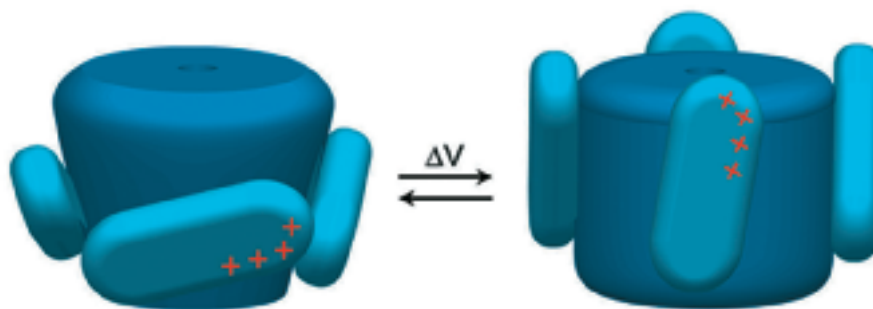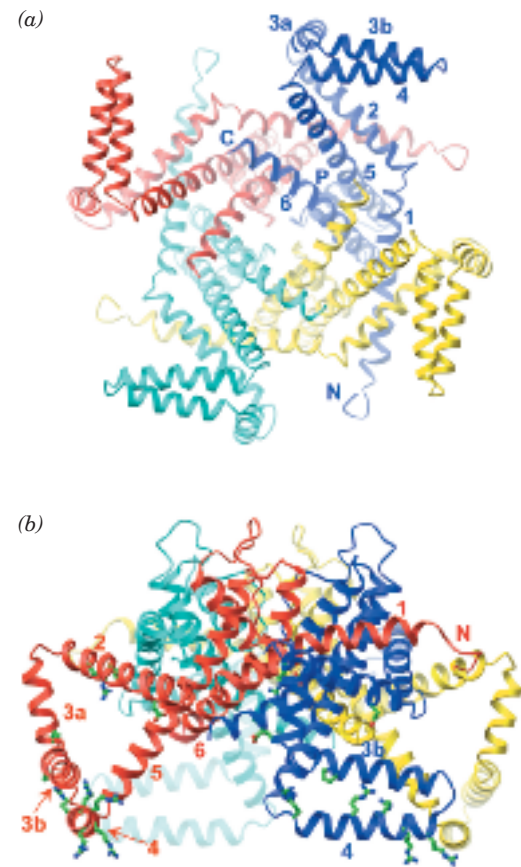
**Figure 1O-12  Model for gating in K$_v$ channels.**    Under the influence of an increase in membrane potential (Na$^+$ flowing into the cell), gating charges (*red plus signs*) are carried through the membrane from inside (*bottom*) to outside (*top*) by the motion of voltage-sensor paddles though the lipid membrane. This motion, it is postulated, opens the pore. [Courtesy of Roderick MacKinnon, Rockefeller University.]

**Figure 10-13  Composite model for the closure of the K$_v$ channel.**    The view is from within the membrane with its extracellular surface above. The bottom portion of the drawing shows a C$_\alpha$ diagram of the X-ray structure of the T1 tetramer with each subunit in a different color (only three of the four subunits are shown for clarity). Only the inactivation peptide that is linked to the red T1 subunit is shown (*yellow*). The upper portion of the drawing represents the K$_v$ channel's transmembrane domain with helices S5 and S6 shown as the X-ray structure of the homologous KcsA channel (Fig. 10-7) and helices S1 to S4 represented schematically. The C-terminal domains, which follow helices S6, have been omitted for clarity. The light green box highlights the selectivity filter formed by the four P loops. The orange box highlights the region occupied by the putative lateral windows through which both the cytoplasmic K$^+$ ions and the inactivation peptides gain access to the central pore. [Courtesy of Senyon Choe, The Salk Institute, La Jolla, California. PDBids for T1 and for the inactivation peptides: 1EQE and 1ZTN.]
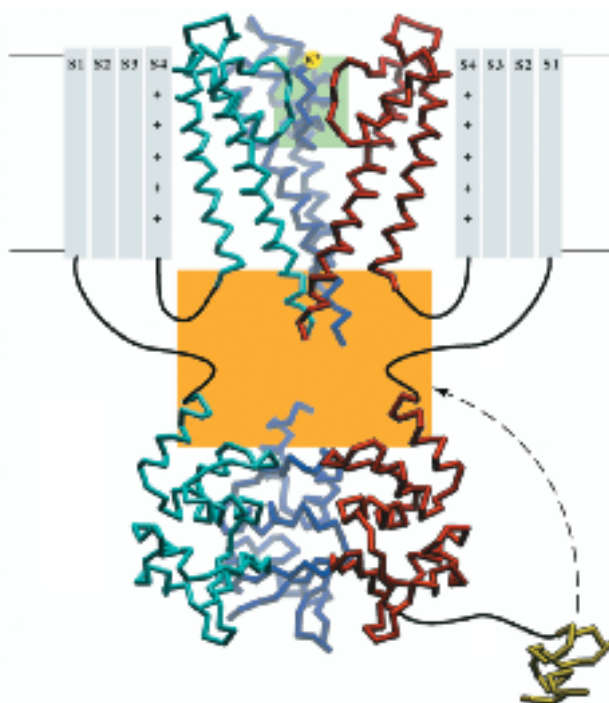


forms a ball-like structure. In the intact K$_V$ channel, this "inactivation ball" is tethered to the end of a flexible 65-residue peptide segment, suggesting that channel inactivation normally occurs when the ball swings around to bind in the mouth of the open K$^+$ pore, thereby blocking the passage of K$^+$ ions. This ball-and-chain model for inactivation is shown schematically in Fig. 10-13.

The X-ray structure of isolated T1 domains reveals that they form a rotationally symmetric homotetrameric structure that is presumably coaxial with the tetrameric pore in the intact K$_V$ channel (Fig. 10-13). The T1 domains in a tetramer do not separate far enough to admit the inactivation peptide, as was demonstrated by the observation that cross-linking these T1 domains together such that they cannot separate does not affect the K$_V$ channel's gating properties. Evidently, the inactivation peptide finds its way into the pore through side windows between the T1 tetramer and the central pore (Fig. 10-13).

The cytoplasmic entrance to the K$^+$ channel pore is only 6 Å in diameter, too narrow to admit the ball. Therefore, it appears that the ball peptide must unfold in order to enter the pore. The first 10 residues of the unfolded ball peptide are predominantly hydrophobic and make contact with the hydrophobic residues lining the K$_V$ channel pore. The next 10 residues, which are largely hydrophilic and contain several basic groups, bind to acidic groups near the pore entrance. Thus, the inactivation peptide acts more like a snake than a ball and chain. A K$_V$ channel engineered so that only one subunit has an inactivation peptide still becomes inactivated but at one-fourth the rate of normal K$_V$ channels. Apparently, any of the normal K$_V$ channel's four inactivation peptides can block the channel and it is simply a matter of chance as to which one does so.

**Other Voltage-Gated Cation Channels Contain a Central Pore.**    Voltage-gated Na$^+$ and Ca$^{2+}$ channels appear to resemble K$^+$ channels, although rather than forming homotetramers, they are monomers of four consecutive do-

mains, each of which is homologous to the $K^+$ channel, separated by often large cytoplasmic loops. These domains presumably assume a pseudotetrameric arrangement about a central pore resembling that of voltage-gated $K^+$ channels. This structural homology suggests that voltage-gated ion channels share a common architecture in which differences in ion selectivity arise from precise stereochemical variations within the central pore. However, outside of their conserved transmembrane core, voltage-gated ion channels with different ion selectivities are highly divergent. For example, the T1 domain of $K_V$ channels is absent in other types of voltage-gated ion channels.

**$Cl^-$ Channels Differ from Cation Channels.**   **$Cl^-$ channels,** which occur in all cell types, permit the transmembrane movement of chloride ions along their concentration gradient. In mammals, the extracellular $Cl^-$ concentration is ~120 mM and the intracellular concentration is ~4 mM.

**ClC $Cl^-$ channels** form a large family of anion channels that occur widely in both prokaryotes and eukaryotes. The X-ray structures of ClC $Cl^-$ channels from two species of bacteria, determined by MacKinnon, reveal, as biophysical measurements had previously suggested, that ClC $Cl^-$ channels are homodimers with each subunit forming an anion-selective pore (Fig. 10-14). Each subunit consists mainly of 18 mostly transmembrane $\alpha$ helices that are remarkably tilted with respect to the membrane plane and have variable lengths compared to the transmembrane helices in other integral proteins of known structures (Section 9-3A).

The specificity of the $Cl^-$ channel results from an electrostatic field established by basic amino acids on the protein surface, which helps funnel anions toward the pore, and by a selectivity filter formed by the N-terminal ends of several $\alpha$ helices. Because the polar groups of an $\alpha$ helix are all aligned (see Fig. 6-7), it forms a strong electrical dipole with its N-terminal
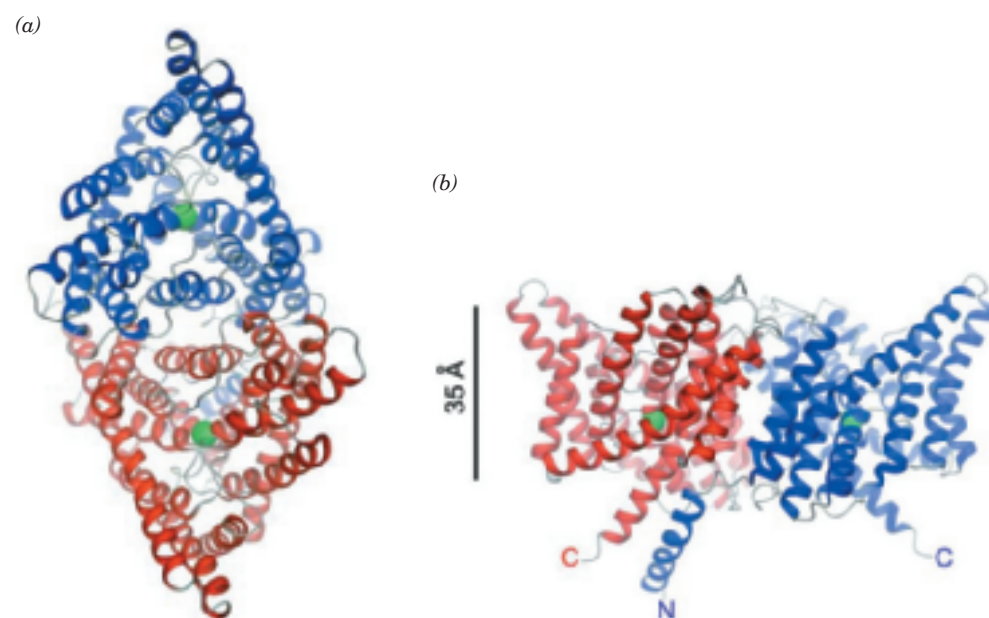
*(a)*

*(b)*



**Figure 10-14   X-Ray structure of the ClC $Cl^-$ channel from *Salmonella typhimurium*.**   Each subunit of the homodimer contains 18 $\alpha$ helices of variable lengths. (*a*) View from the extracellular side of the membrane. The two subunits are colored blue and red. The green spheres represent $Cl^-$ ions in the selectivity filter. (*b*) View from within the membrane with the extracellular surface above. The scale bar indicates the thickness of the membrane. [Courtesy of Roderick MacKinnon, Rockefeller University. PDBid 1KPL.]

end positively charged. This feature of the selectivity filter helps attract $Cl^-$ ions, which are specifically coordinated by main chain amide nitrogens and side chain hydroxyls from Ser and Tyr residues (recall that a $K^+$ ion in the central cavity of a KscA channel interacts with the C-terminal ends of $\alpha$ helices; Fig. 10-7c). A positively charged residue such as Lys or Arg, if it were present in the selectivity filter, would probably bind a $Cl^-$ ion too tightly to facilitate its rapid transit through the channel.

Unlike the $K^+$ channel, which has a central aqueous cavity (Fig. 10-7c), the $Cl^-$ channel is hourglass-shaped, with its narrowest part in the center of the membrane and flanked by wider aqueous "vestibules." A conserved Glu side chain projects into the pore. This group would repel other anions, suggesting that rapid $Cl^-$ flux requires a protein conformational change in which the Glu side chain moves aside. Another anion could push the Glu away, which explains why some $Cl^-$ channels appear to be activated by $Cl^-$ ions; that is, they open in response to a certain concentration of $Cl^-$ in the extracellular fluid.

## D  Aquaporins

The observed rapid passage of water molecules across biological membranes had long been assumed to occur via simple diffusion that was made possible by the small size of water molecules and their high concentrations in biological systems. However, certain cells, such as those in the kidney, can sustain particularly rapid rates of water transport, which can be reversibly inhibited by mercuric ions. This suggested the existence of previously unrecognized protein pores that conduct water through biological membranes. The first of these elusive proteins was discovered in 1992 by Peter Agre, who named them **aquaporins.**

Aquaporins are widely distributed in nature; plants may have as many as 50 different aquaporins. The seven mammalian aquaporins that have been identified are expressed at high levels in tissues that rapidly transport water, including kidneys, salivary glands, and lacrimal glands (which produce tears). Aquaporins permit the passage of water molecules at an extremely high rate ($\sim 3 \times 10^9$ per second) but do not permit the transport of solutes (e.g., glycerol or urea) or ions, including, most surprisingly, protons (really hydronium ions; $H_3O^+$), whose free passage would discharge the cell's membrane potential.

The most extensively characterized member of the aquaporin family, **AQP1,** is a homotetrameric glycoprotein. Its X-ray and electron crystallographic structures reveal that each of its subunits consists mainly of six transmembrane $\alpha$ helices plus two shorter helices that lie within the bilayer (Fig. 10-15). These helices are arranged so as to form an elongated hourglass-shaped central pore that, at its narrowest point, the so-called constriction region, is $\sim 2.8$ Å wide, which is the van der Waals diameter of a water molecule (Fig. 10-16). Much of the pore is lined with hydrophobic groups whose lack of strong interactions with water molecules facilitates the rapid passage of water through the pore. However, for a water mole-
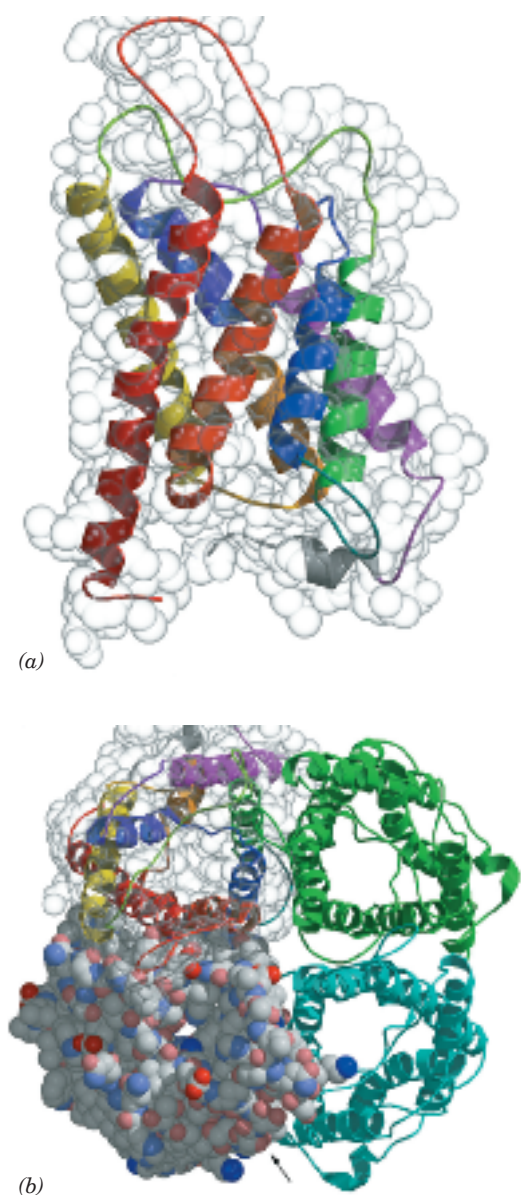


(a)



(b)

**Figure 10-15   X-Ray structure of the aquaporin AQP1 from bovine erythrocytes.**
(a) Superimposed ribbon and space-filling models of an aquaporin subunit as viewed from within the membrane with its extracellular surface above. The eight helical segments are drawn with different colors. (b) View of the aquaporin tetramer from the extracellular surface. Each subunit forms a water-transport channel, which is visible in the space-filling subunit model at the lower left. [Courtesy of Bing Jap, University of California at Berkeley. PDBid 1J4N.]

cule to transit the constriction region, it must shed its associated waters of hydration. This is facilitated by the side chains of highly conserved Arg and His residues as well as several backbone carbonyl groups, all of which line the constriction region. These groups are oriented so as to form hydrogen bonds to a transiting water molecule and hence readily displace its associated water molecules, much as occurs with $K^+$ in the selectivity filter of the KcsA channel (Section 10-2C).

If water were to pass through aquaporin as an uninterrupted chain of hydrogen-bonded molecules, this would facilitate the even more rapid passage of protons through the channel via proton jumping (Section 2-2A; in order for more than one such series of proton jumps to occur, each water molecule in the chain must reorient such that one of its protons forms a hydrogen bond to the next water molecule in the chain). However, aquaporin interrupts this process by forming hydrogen bonds from the side chain $NH_2$ groups of two highly conserved Asn residues to a water molecule that is centrally located in the pore (Fig. 10-16). Consequently, although this central water molecule can readily donate hydrogen bonds to its neighboring water molecules in the hydrogen bonded chain, it cannot accept one from them nor reorient, thereby severing the "proton-conducting wire" (Fig. 2-15).

## E  Transport Proteins

Up to this point, we have examined the structures and functions of membrane proteins that form a physical passageway for small molecules, ions, or water. Membrane proteins known as **connexins** also form such channels, in the form of **gap junctions** between cells (see Box 10-1). However, not all membrane transport proteins offer a discrete bilayer-spanning pore. Instead, some proteins undergo conformational changes to move substances from one side of the membrane to the other. The **erythrocyte glucose transporter** (also known as **GLUT1**) is such a protein.

Biochemical evidence indicates that GLUT1 has glucose binding sites on both sides of the membrane. John Barnett showed that adding a propyl group to glucose C1 prevents glucose binding to the outer surface of the membrane, whereas adding a propyl group to C6 prevents binding to the inner surface. He therefore proposed that this transmembrane protein has two alternate conformations: one with the glucose site facing the external cell surface, requiring O1 contact and leaving O6 free, and the other with the glucose site facing the internal cell surface, requiring O6 contact and leaving O1 free. Transport apparently occurs as follows (Fig. 10-17):

1. Glucose binds to the protein on one face of the membrane.
2. A conformational change closes the first binding site and exposes the binding site on the other side of the membrane (transport).
3. Glucose dissociates from the protein.
4. The transport cycle is completed by the reversion of GLUT1 to its initial conformation in the absence of bound glucose (recovery).

This transport cycle can occur in either direction, according to the relative concentrations of intracellular and extracellular glucose. GLUT1 provides
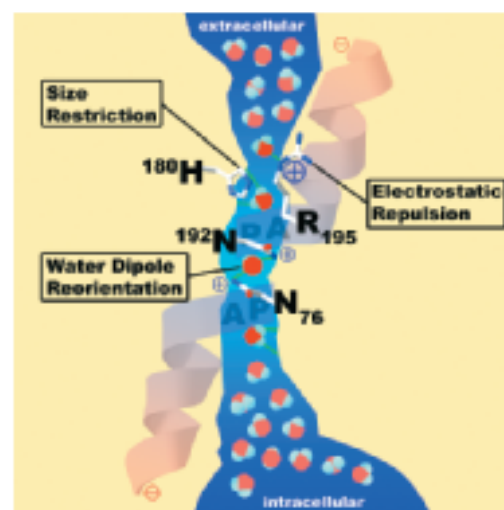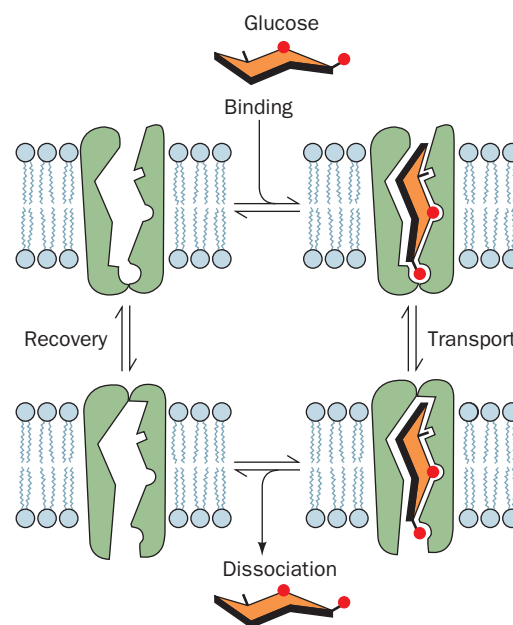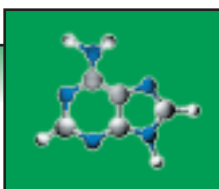


Figure 1O-16  **Schematic model of the water-conducting pore of aquaporin AQP1 viewed from within the membrane with the extracellular surface above.** The positions of residues critical for preventing the passage of protons, other ions, and small molecule solutes are indicated. [Courtesy of Peter Agre, The Johns Hopkins School of Medicine.]



Figure 1O-17  *Key to Function.*  **Model for glucose transport.**  The transport protein alternates between two mutually exclusive conformations. Glucose binds on one side of the membrane and is released on the other side after the protein conformation changes. The glucose molecule (*red*) is not drawn to scale. [After Baldwin, S.A. and Lienhard, G.E., *Trends Biochem. Sci.* **6,** 210 (1981).]  See the Animated Figures.

# BOX 10-1

## Perspectives in Biochemistry

### Gap Junctions

Most eukaryotic cells are in metabolic as well as physical contact with neighboring cells. This contact is brought about by tubular particles, named **gap junctions,** that join discrete regions of neighboring plasma membranes much like hollow rivets. The gap junction consists of two apposed plasma membrane–embedded complexes. Small molecules and ions, but not macromolecules, can pass between cells via the gap junction's central channel.
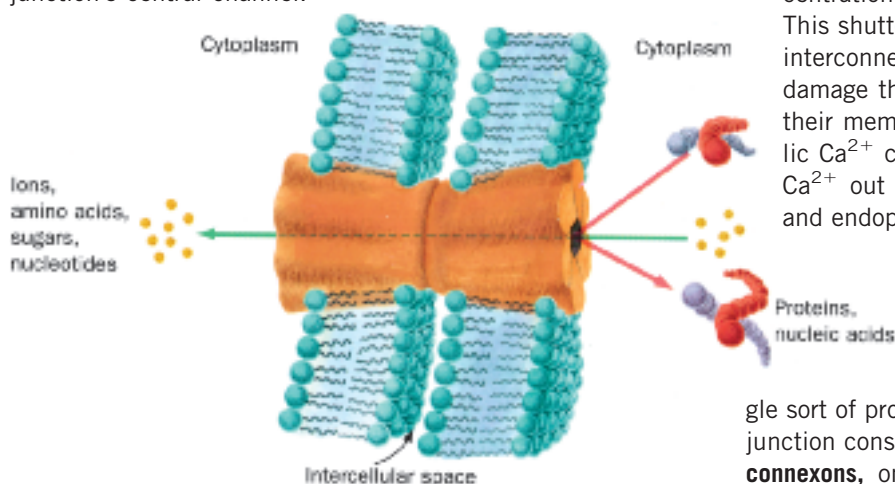


These intercellular channels are so widespread that many whole organs are continuous from within. Thus, *gap junctions are important intercellular communication channels.* For example, the synchronized contraction of heart muscle is brought about by flows of ions through gap junctions, and gap junctions serve as conduits for some of the substances that mediate embryonic development.

Mammalian gap junction channels are 16 to 20 Å in diameter, which Werner Loewenstein established by microinjecting single cells with fluorescent molecules of various sizes and observing with a fluorescence microscope whether the fluorescent probe passed into neighboring cells. The mole-cules and ions that can pass freely between neighboring cells are limited in molecular mass to a maximum of $\sim$1000 D; macromolecules such as proteins and nucleic acids cannot leave a cell via this route.

The diameter of a gap junction channel varies with $Ca^{2+}$ concentration: The channels are fully open when the $Ca^{2+}$ level is $<10^{-7}$ M and become narrower as the $Ca^{2+}$ concentration increases until, above $5 \times 10^{-5}$ M, they close. This shutter system is thought to protect communities of interconnected cells from the otherwise catastrophic damage that would result from the death of even one of their members. Cells generally maintain very low cytosolic $Ca^{2+}$ concentrations ($<10^{-7}$ M) by actively pumping $Ca^{2+}$ out of the cell as well as into their mitochondria and endoplasmic reticulum (Section 10-3B). $Ca^{2+}$ floods back into leaky or metabolically depressed cells, thereby inducing closure of their gap junctions and sealing them off from their neighbors.

Gap junctions are constructed from a single sort of protein subunit known as a **connexin.** A single gap junction consists of two hexagonal rings of connexins, called **connexons,** one from each of the adjoining plasma membranes. A given animal expresses numerous genetically distinct connexins, with molecular masses ranging from 25 to 50 kD. At least some connexons may be formed from two or more species of connexins, and the gap junctions joining two cells may consist of two different types of connexons. These various types of gap junctions presumably differ in their selectivities for the substances they transmit.

The structure of a cardiac gap junction, determined by electron crystallography, reveals a symmetrical assembly that has a diameter of $\sim$70 Å, a length of $\sim$150 Å, and encloses a central channel whose diameter varies from $\sim$40 Å at its mouth to $\sim$15 Å in its interior. The transmembrane portions of the gap junction each contain 24 rods of electron density

a means of equilibrating the glucose concentration across the erythrocyte membrane without any accompanying leakage of small molecules or ions (as might occur through an always-open channel such as a porin).

*All known transport proteins appear to be asymmetrically situated transmembrane proteins that alternate between two conformational states in which the ligand-binding sites are exposed, in turn, to opposite sides of the membrane.* Such a mechanism is analogous to the T → R allosteric transition of proteins such as hemoglobin (Section 7-3). In fact, many of the features of

that are arranged with hexagonal symmetry and which extend normal to the membrane plane.
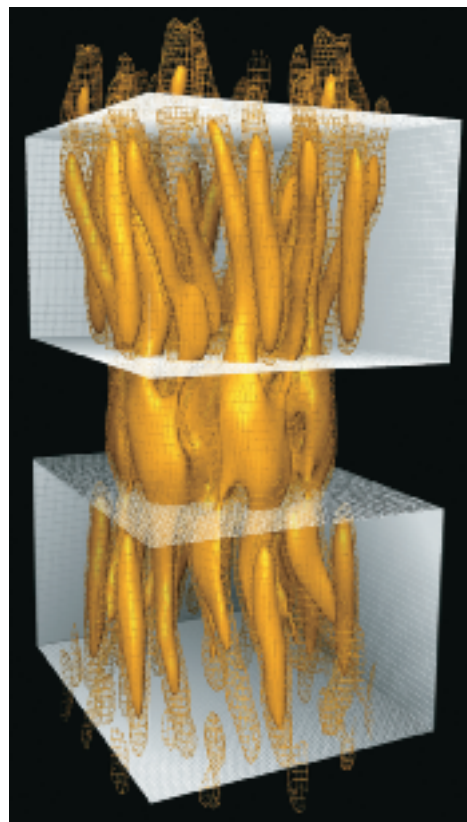


Here, the electron density at two different levels is represented by the solid and mesh contours (*gold*), whereas the white boxes indicate the positions of the cell membranes.

[Electron crystal structure courtesy of Mark Yeager, The Scripps Research Institute, La Jolla, California.]

ligand-binding proteins such as myoglobin and hemoglobin also apply to transport proteins (see Box 10-2).

Sequence analysis indicates that GLUT1 has 12 membrane-spanning α helices. This protein belongs to a large family of transporters whose structures have not been as well characterized as those of channel-type proteins. The 6.5-Å resolution electron crystal structure of a bacterial **oxalate transporter** named **OxlT** reveals that its 12 transmembrane helices are arranged around a central cavity, which presumably represents a substrate-binding
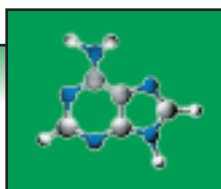
## BOX 10-2

# *Perspectives in Biochemistry*

### *Differentiating Mediated and Nonmediated Transport*

Glucose and many other compounds can enter cells by a nonmediated pathway; that is, they slowly diffuse into cells at a rate proportional to their membrane solubility and their concentrations on either side of the membrane. This is a linear process: The **flux** (rate of transport per unit area) of a substance across the membrane increases with the magnitude of its concentration gradient (the difference between its internal and external concentrations). If the same substance, say glucose, moves across a membrane by means of a transport protein, its flux is no longer linear. This is one of four characteristics that distinguish mediated from nonmediated transport:

1. **Speed and specificity.** The solubilities of the chemically similar sugars D-glucose and D-mannitol in a synthetic lipid bilayer are similar. However, the rate at which glucose moves through the erythrocyte membrane is four orders of magnitude faster than that of D-mannitol. The erythrocyte membrane must therefore contain a system that transports glucose and that can distinguish D-glucose from D-mannitol.

2. **Saturation.** The rate of glucose transport into an erythrocyte does not increase infinitely as the external glucose concentration increases: The rate gradually approaches a maximum. Such an observation is evidence that a specific number of sites on the membrane are involved in the transport of glucose. At high [glucose], the transporters become saturated, much like myoglobin becomes saturated with $O_2$ at high $pO_2$ (Fig. 7-4). As expected, the following plot of glucose flux versus [glucose] is hyperbolic.
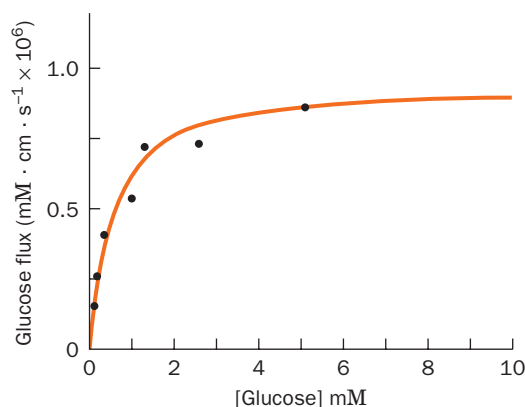
The nonmediated glucose flux increases linearly with [glucose] but would not visibly depart from the baseline on the scale of the above graph.

3. **Competition.** The above curve is shifted to the right in the presence of a substance that competes with glucose for binding to the transporter; for example, 6-*O*-benzyl-D-galactose has this effect. Competition is not a feature of nonmediated transport, since no transport protein is involved.

4. **Inactivation.** Reagents that chemically modify proteins and hence may affect their functions may eliminate the rapid, saturable flux of glucose into the erythrocyte. The susceptibility of the erythrocyte glucose transport system to protein-modifying reagents is additional proof that it is a protein.

[Graph based on data from Stein, W.D., *Movement of Molecules across Membranes*, p. 134, Academic Press (1967).]

---
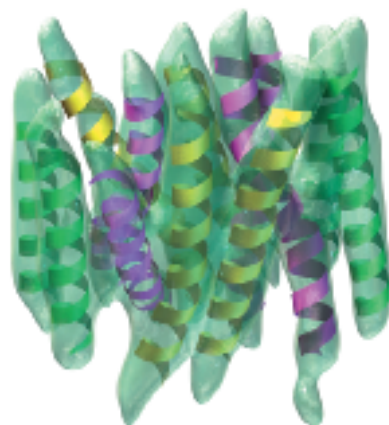
site (Fig. 10-18). The protein exhibits a high degree of symmetry between its cytoplasmic and external halves, which is consistent with its ability to transport substances both into and out of the cell. The structure shown in Fig. 10-18 probably corresponds to a conformational intermediate that is not fully accessible to either the cytoplasmic or extracellular face of the membrane.

**Figure 10-18**   **Electron crystal structure of oxalate transporter OxlT from *Oxalobacter formigenes.*** Twelve α helices have been fitted to the electron density map, which has a resolution of 6.5 Å. The green helices are nearly perpendicular to the plane of the membrane; yellow helices include a bend; and magenta helices are both bent and curved to match the electron density. Segments linking the helices are not resolved. [Courtesy of Sriram Subramaniam, NIH, Bethesda, Maryland.]

Some transporters can transport more than one substance. For example, the bacterial oxalate transporter transports **oxalate** into the cell and transports **formate** out.

$$^-OOC-COO^- \qquad H-COO^-$$
**Oxalate** $\qquad$ **Formate**

Some transport proteins move more than one substance at a time. Hence, it is useful to categorize mediated transport according to the stoichiometry of the transport process (Fig. 10-19):

1. A **uniport** involves the movement of a single molecule at a time. GLUT1 is a uniport system.
2. A **symport** simultaneously transports two different molecules in the same direction.
3. An **antiport** simultaneously transports two different molecules in opposite directions.



**Figure 10-19** **Uniport, symport, and antiport translocation systems.**

## 3 | Active Transport

Passive-mediated transporters, including porins, ion channels, and proteins such as GLUT1, facilitate the transmembrane movement of substances according to the relative concentrations of the substance on either side of the membrane. For example, the glucose concentration in the blood plasma ($\sim$5 mM) is generally higher than in cells, so GLUT1 allows glucose to enter the erythrocyte to be metabolized. Many substances, however, are available on one side of a membrane in lower concentrations than are required on the other side of the membrane. Such substances must be actively and selectively transported across the membrane against their concentration gradients.

Active transport is an endergonic process that, in most cases, is coupled to the hydrolysis of ATP. The elucidation of the mechanism by which the chemical energy released from ATP is used to drive a mechanical process has been a challenging biochemical problem. In this section, we examine membrane-bound ATPases that translocate cations; these proteins carry out **primary active transport.** In **secondary active transport,** the free energy of the electrochemical gradient generated by another mechanism, such as an ion-pumping ATPase, is used to transport a neutral molecule against its concentration gradient.

### A  (Na$^+$–K$^+$)–ATPase

One of the most thoroughly studied active transport systems is the **(Na$^+$–K$^+$)–ATPase** in the plasma membranes of higher eukaryotes, which was first characterized by Jens Skou. This transmembrane protein consists of two types of subunits: a 110-kD nonglycosylated $\alpha$ subunit that contains the enzyme's catalytic activity and ion-binding sites, and a 55-kD glycoprotein $\beta$ subunit of unknown function. Sequence analysis suggests that the $\alpha$ subunit has eight transmembrane $\alpha$-helical segments and two large cytoplasmic domains. The $\beta$ subunit has a single transmembrane helix and a large extracellular domain. The protein may function as an $(\alpha\beta)_2$ tetramer *in vivo* (Fig. 10-20).

**Figure 10-20** **(Na$^+$–K$^+$)–ATPase.**   This diagram shows the transporter's putative dimeric structure and its orientation in the plasma membrane. Cardiotonic steroids (Box 10-3) bind to the external surface of the transporter, thereby inhibiting transport.
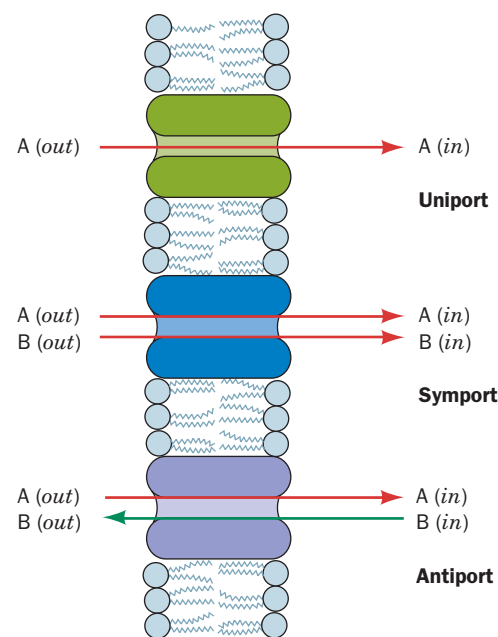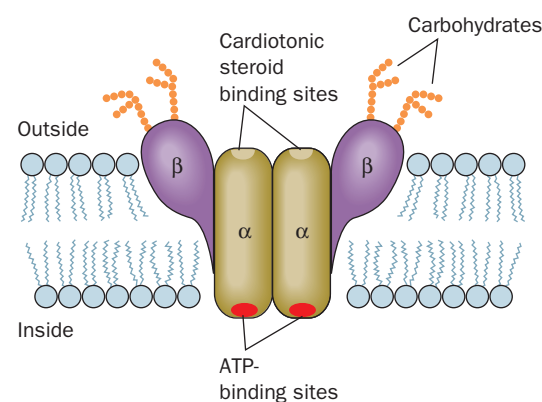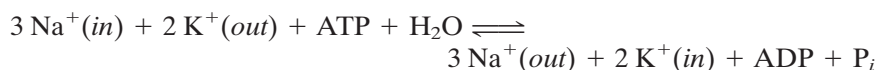
The $(Na^+-K^+)$–ATPase is often called the **$(Na^+-K^+)$ pump** because it pumps $Na^+$ out of and $K^+$ into the cell with the concomitant hydrolysis of intracellular ATP. The overall stoichiometry of the reaction is

$$3\,Na^+(in) + 2\,K^+(out) + ATP + H_2O \rightleftharpoons$$
$$3\,Na^+(out) + 2\,K^+(in) + ADP + P_i$$

The $(Na^+-K^+)$–ATPase is an antiport that generates a charge separation across the membrane, since three positive charges exit the cell for every two that enter. This extrusion of $Na^+$ enables animal cells to control their water content osmotically; *without functioning $(Na^+-K^+)$–ATPases to maintain a low internal $[Na^+]$, water would osmotically rush in to such an extent that animal cells, which lack cell walls, would swell and burst.* The electrochemical gradient generated by the $(Na^+-K^+)$–ATPase is also responsible for the electrical excitability of nerve cells (Section 10-2C). In fact, all cells expend a large fraction of the ATP they produce (up to 70% in nerve cells) to maintain their required cytosolic $Na^+$ and $K^+$ concentrations.

The key to the $(Na^+-K^+)$–ATPase is the phosphorylation of a specific Asp residue of the transport protein. ATP phosphorylates the transporter only in the presence of $Na^+$, whereas the resulting aspartyl phosphate residue

$$\begin{array}{c} | \\ C{=}O \qquad\quad O \\ | \qquad\qquad\quad || \\ CH{-}CH_2{-}C{-}OPO_3^- \\ | \\ NH \\ | \end{array}$$
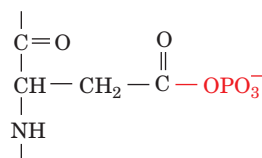
**Aspartyl phosphate
residue**

is subject to hydrolysis only in the presence of $K^+$. This suggests that the $(Na^+-K^+)$–ATPase has two conformational states (called $E_1$ and $E_2$) with different structures, different catalytic activities, and different ligand specificities. The protein appears to operate in the following manner (Fig. 10-21):

1. The transporter in the $E_1$ state binds three $Na^+$ ions inside the cell and then binds ATP to yield an $E_1 \cdot ATP \cdot 3\,Na^+$ complex.
2. ATP hydrolysis produces ADP and a "high-energy" aspartyl phosphate intermediate $E_1{\sim}P \cdot 3\,Na^+$ (here "$\sim$" indicates a "high-energy" bond).
3. This "high-energy" intermediate relaxes to its "low-energy" conformation, $E_2{-}P \cdot 3\,Na^+$, and releases its bound $Na^+$ outside the cell.
4. $E_2{-}P$ binds two $K^+$ ions from outside the cell to form an $E_2{-}P \cdot 2\,K^+$ complex.
5. The phosphate group is hydrolyzed, yielding $E_2 \cdot 2\,K^+$.
6. $E_2 \cdot 2\,K^+$ changes conformation, releases its two $K^+$ ions inside the cell, and replaces them with three $Na^+$ ions, thereby completing the transport cycle.

Although each of the above reaction steps is individually reversible, the cycle, as diagramed in Fig. 10-21, circulates only in the clockwise direction under normal physiological conditions. This is because ATP hydrolysis and ion transport are coupled vectorial (unidirectional) processes. The vectorial nature of the reaction cycle results from the alternation of some of
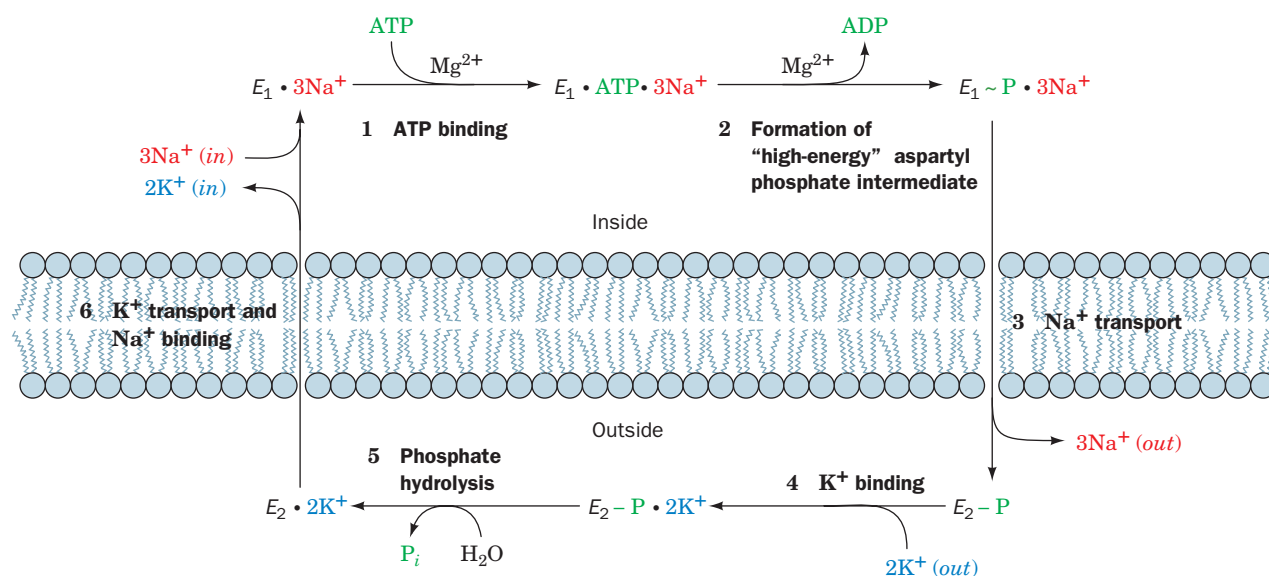
**Figure 10-21** *Key to Function.* Scheme for the active transport of Na$^+$ and K$^+$ by the (Na$^+$–K$^+$)–ATPase.

the steps of the exergonic ATP hydrolysis reaction (Steps 1 + 2 and Step 5) with some of the steps of the endergonic ion transport process (Steps 3 + 4 and Step 6). Thus, *neither reaction can go to completion unless the other one also does*. Study of the (Na$^+$–K$^+$)–ATPase has been greatly facilitated by the use of glycosides that inhibit the transporter (see Box 10-3).

## B Ca$^{2+}$–ATPase

Transient increases in cytosolic [Ca$^{2+}$] trigger numerous cellular responses including muscle contraction (Section 28-2B), the release of neurotransmitters, and glycogen breakdown (Section 15-3). Moreover, Ca$^{2+}$ is an important activator of oxidative metabolism (Section 17-4).

The [Ca$^{2+}$] in the cytosol (~0.1 μM) is four orders of magnitude less than it is in the extracellular spaces [~1500 μM; intracellular Ca$^{2+}$ might otherwise combine with phosphate to form Ca$_3$(PO$_4$)$_2$, which has a maximum solubility of only 65 μM]. This large concentration gradient is maintained by the active transport of Ca$^{2+}$ across the plasma membrane and the endoplasmic reticulum (the sarcoplasmic reticulum in muscle) by a **Ca$^{2+}$–ATPase (Ca$^{2+}$ pump)** that actively pumps two Ca$^{2+}$ ions out of the cytosol at the expense of ATP hydrolysis, while countertransporting two or three protons. The mechanism of the Ca$^{2+}$–ATPase (Fig. 10-22) resembles that of the (Na$^+$–K$^+$)–ATPase (Fig. 10-21).

The superimposed X-ray structures of the Ca$^{2+}$–ATPase from rabbit muscle sarcoplasmic reticulum in its E$_1$ and E$_2$ confor-
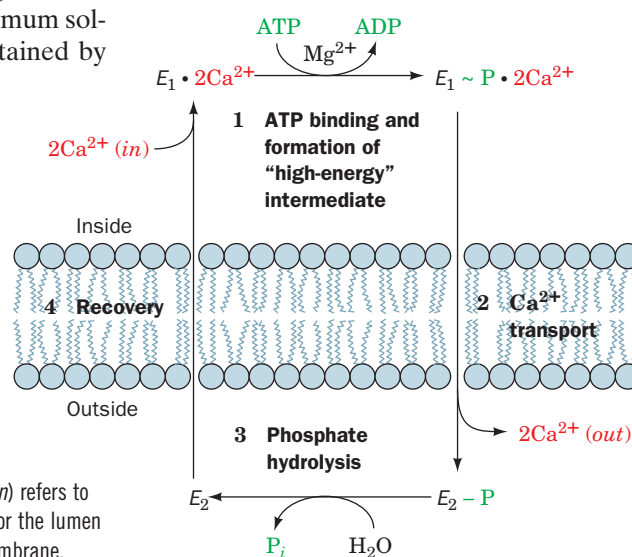


**Figure 10-22** Scheme for the active transport of Ca$^{2+}$ by the Ca$^{2+}$–ATPase. Here (*in*) refers to the cytosol and (*out*) refers to the outside of the cell for plasma membrane Ca$^{2+}$–ATPase or the lumen of the endoplasmic reticulum (or sarcoplasmic reticulum) for the Ca$^{2+}$–ATPase of that membrane.
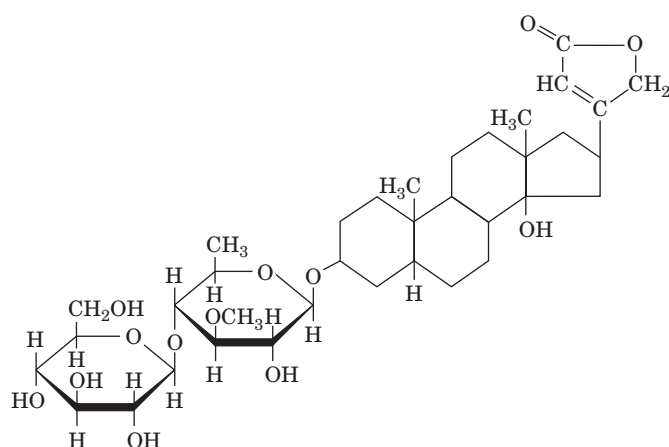
# BOX 10-3

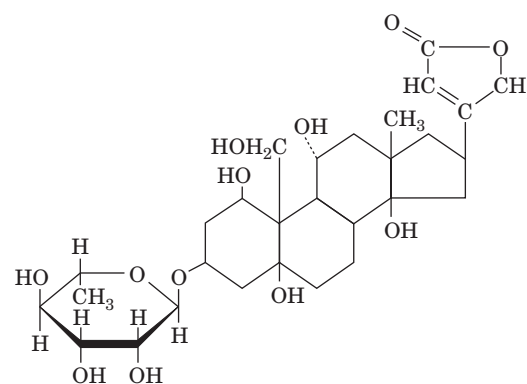## Biochemistry in Health and Disease

### The Action of Cardiac Glycosides

The cardiac glycosides are natural products that increase the intensity of heart muscle contraction. Indeed, **digitalis,** an extract of purple foxglove leaves, which contains a mixture of cardiac glycosides including **digitoxin** (**digitalin;** see figure below), has been used to treat congestive heart failure for centuries. The cardiac glycoside **ouabain** (pronounced wabane), a product of the East African ouabio tree, has been long used as an arrow poison.

10-21. The resultant increase in intracellular $[Na^+]$ stimulates the cardiac ($Na^+$–$Ca^{2+}$) antiport system, which pumps $Na^+$ out of and $Ca^{2+}$ into the cell, ultimately boosting the $[Ca^{2+}]$ in the sarcoplasmic reticulum. Thus, the release of $Ca^{2+}$ to trigger muscle contraction (Section 28-2B) produces a larger than normal increase in cytosolic $[Ca^{2+}]$, thereby intensifying the force of cardiac muscle contraction. Ouabain, which was once thought to be produced only by plants, has

**Digitoxin (digitalin)**

**Ouabain**

These two steroids, which are still among the most commonly prescribed cardiac drugs, inhibit the ($Na^+$–$K^+$)–ATPase by binding strongly to an externally exposed portion of the protein (Fig. 10-20) so as to block Step 5 in Fig.

recently been discovered to be an animal hormone that is secreted by the adrenal cortex and functions to regulate cellular $[Na^+]$ and overall body salt and water balance.
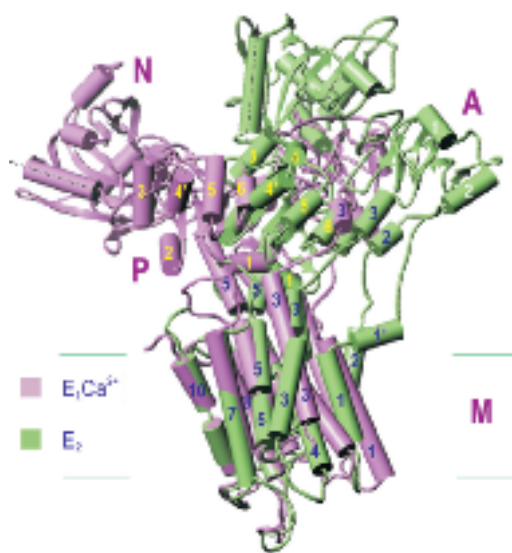


mations, determined by Chikashi Toyoshima, are shown in Fig. 10-23. Two $Ca^{2+}$ ions bind within a bundle of 10 transmembrane helices. Three additional domains form a large structure on the cytoplasmic side of the membrane. The differences between the $Ca^{2+}$-bound ($E_1$) and the $Ca^{2+}$-free ($E_2$) structures indicate that the transporter undergoes extensive re-

**Figure 10-23** **X-Ray structures of the $Ca^{2+}$-free and $Ca^{2+}$-bound $Ca^{2+}$–ATPase.** The $Ca^{2+}$-free form, $E_2$, is green with black helix numbers, and the $Ca^{2+}$-bound form, $E_1Ca^{2+}$, is violet with yellow helix numbers. These proteins, which are superimposed on their transmembrane domains, are viewed from within the membrane with the cytosolic side up. Ten transmembrane helices form the M (for membrane) domain, ATP binds to the N (for nucleotide-binding) domain, the Asp residue that is phosphorylated during the reaction cycle is located on the P (for phosphorylation) domain, and the A (for actuator) domain is so named because it participates in the transmission of major conformational changes. A dashed line highlights the orientation of a helix in the N domain in the two conformations and the horizontal lines delineate the membrane. [Courtesy of Chikashi Toyoshima, University of Tokyo, Japan. PDBids 1EUL and 1WIO.]

arrangements, particularly in the positions of the cytoplasmic domains, but also in the $Ca^{2+}$-transporting membrane domain, during the reaction cycle. These changes apparently mediate communication between the $Ca^{2+}$ binding sites and the ~80-Å-distant site where bound ATP is hydrolyzed.

## C   Ion Gradient–Driven Active Transport

Systems such as the $(Na^+–K^+)$–ATPase generate electrochemical gradients across membranes. The free energy stored in an electrochemical gradient (Eq. 10-3) can be harnessed to power various endergonic physiological processes. For example, cells of the intestinal epithelium take up dietary glucose by $Na^+$-dependent symport (Fig. 10-24). The immediate energy source for this "uphill" transport process is the $Na^+$ gradient. This process is an example of secondary active transport because *the $Na^+$ gradient in these cells is maintained by the $(Na^+–K^+)$–ATPase.* The $Na^+$–glucose transport system concentrates glucose inside the cell. Glucose is then transported into the capillaries through a passive-mediated glucose uniport (which resembles GLUT1; Fig. 10-17). Thus, since glucose enhances $Na^+$ resorption, which in turn enhances water resorption, glucose, in addition to salt and water, should be fed to individuals suffering from salt and water losses due to diarrhea.

**Lactose Permease Requires a Proton Gradient.**   Gram-negative bacteria such as *E. coli* contain several active transport systems for concentrating sugars. One extensively studied system, **lactose permease** (also known as **galactoside permease**), *utilizes the proton gradient across the bacterial cell membrane to cotransport $H^+$ and lactose.* The proton gradient is metabolically generated through oxidative metabolism in a manner similar to that in mitochondria (Section 17-2). The electrochemical potential gradient created by both these systems is used mainly to drive the synthesis of ATP.

Lactose permease is a 417-residue monomer that, like GLUT1 and the oxalate transporter (Section 10-2E), to which it is distantly related, consists largely of 12 transmembrane helices with its N- and C-termini in the cyto-
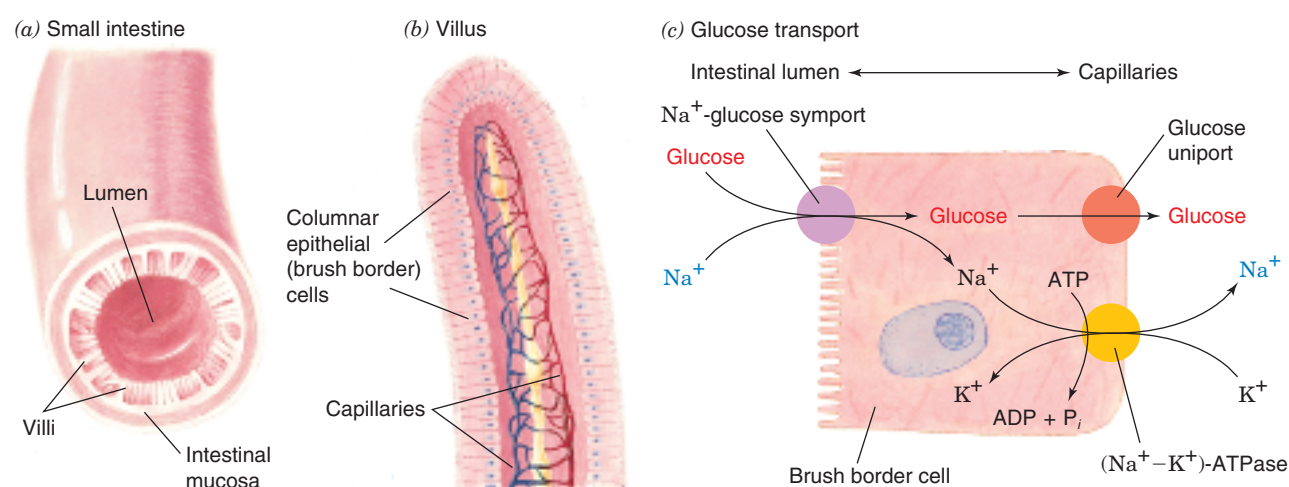


*(a)* Small intestine    *(b)* Villus    *(c)* Glucose transport

**Figure 10-24   Glucose transport in the intestinal epithelium.**   The brushlike villi lining the small intestine greatly increase its surface area (*a*), thereby facilitating the absorption of nutrients. The brush border cells from which the villi are formed (*b*) concentrate glucose from the intestinal lumen in symport with $Na^+$ (*c*), a process that is driven by the $(Na^+–K^+)$–ATPase, which is located on the capillary side of the cell and functions to maintain a low internal $[Na^+]$. The glucose is exported to the bloodstream via a separate passive-mediated uniport system similar to GLUT1.
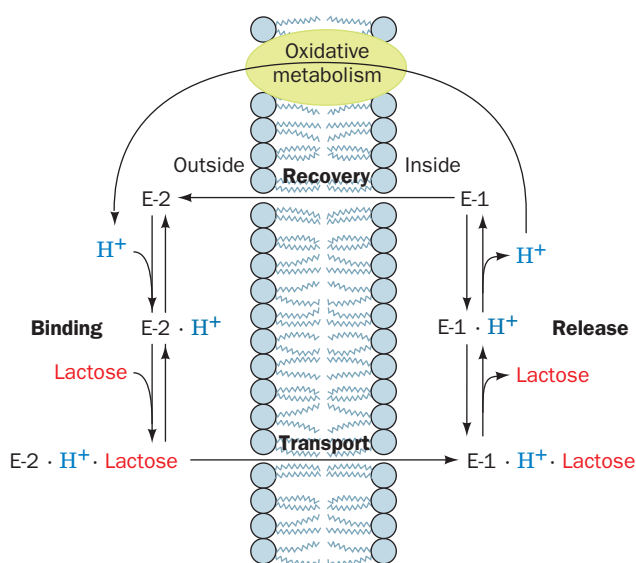
**Figure 10-25   Scheme for the cotransport of H$^+$ and lactose by lactose permease in *E. coli.*** H$^+$ binds first to E-2 outside the cell, followed by lactose. They are sequentially released from E-1 inside the cell. E-2 must bind to lactose and H$^+$ in order to change conformation to E-1, thereby cotransporting these substances into the cell. E-1 changes conformation to E-2 when neither lactose nor H$^+$ is bound, thus completing the transport cycle.

plasm. As does (Na$^+$–K$^+$)–ATPase, it has two major conformational states (Fig. 10-25):

**1.** E-1, which has a low-affinity lactose-binding site facing the interior of the cell.

**2.** E-2, which has a high-affinity lactose-binding site facing the exterior of the cell.

Ronald Kaback established that E-1 and E-2 can interconvert only when their H$^+$ and lactose binding sites are either both filled or both empty. This prevents dissipation of the H$^+$ gradient without cotransport of lactose into the cell. It also prevents transport of lactose out of the cell since this would require cotransport of H$^+$ against its concentration gradient.
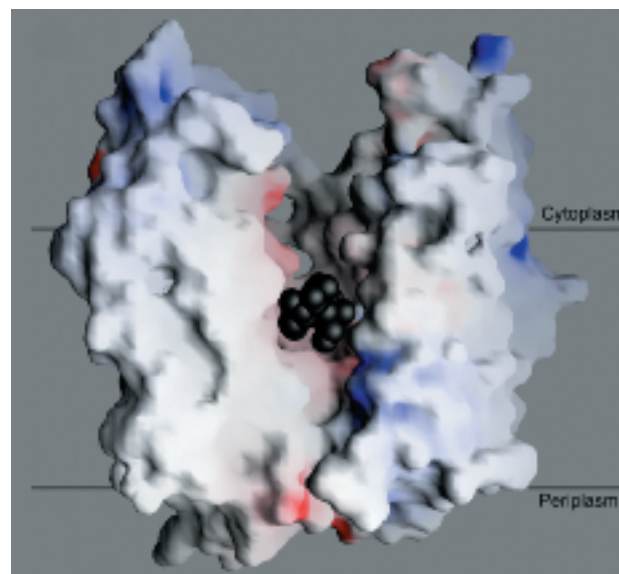
The X-ray structure of lactose permease in complex with a tight-binding lactose analog, determined by Kaback and So Iwata, reveals that this protein consists of two structurally similar and twofold symmetrically positioned domains containing six transmembrane helices each (Fig. 10-26*a*). A large internal hydrophilic cavity is open to the cytoplasmic side of the membrane (Fig. 10-26*b*) so that the structure represents the E-1 state of the protein. The lactose analog is bound in the cavity at a position that is approximately equidistant from both sides of the membrane, consistent with the



*(a)*



*(b)*
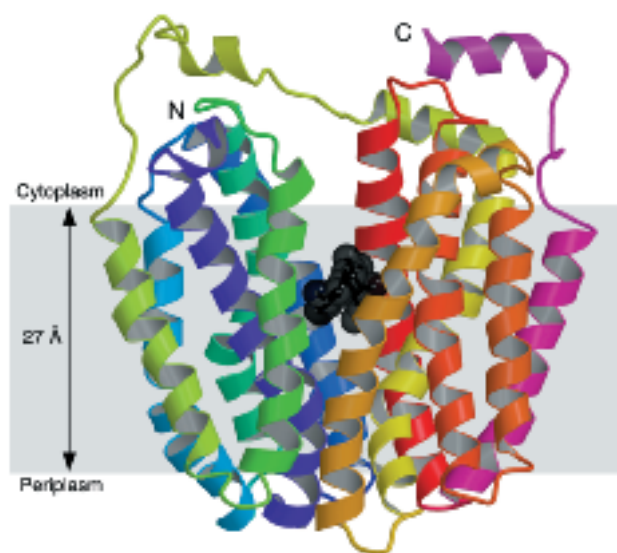
**Figure 10-26   X-Ray structure of lactose permease from *E. coli.***
(*a*) Ribbon diagram as viewed from the membrane with the cytoplasmic side up. The protein's 12 transmembrane helices are colored in rainbow order with the N-terminus purple and the C-terminus pink. The bound lactose analog is represented by black spheres. (*b*) Surface model viewed as in Part *a* but with the two helices closest to the viewer in Part *a* removed to reveal the lactose-binding cavity. The surface is colored according to its electrostatic potential with positively charged areas blue, negatively charged areas red, and neutral areas white. [Courtesy of H. Ronald Kaback, UCLA. PDBid 1PV7.]

model that the lactose binding site is alternately accessible from each side of the membrane (e.g., Fig. 10-17). Arg, His, and Glu residues that mutational studies have implicated in proton translocation are located in the vicinity of the lactose binding site.

## ◉ SUMMARY

1. The mediated and nonmediated transport of a substance across a membrane is driven by its chemical potential difference.

2. Ionophores facilitate ion diffusion by binding an ion, diffusing through the membrane, and then releasing the ion; or by forming a channel.

3. Porins form β barrel structures about a central channel that is selective for anions, cations, or certain small molecules.

4. Ion channels mediate changes in membrane potential by allowing the rapid and spontaneous transport of ions. Ion channels are highly solute-selective and open and close (gate) in response to various stimuli. Nerve impulses involve ion channels.

5. Aquaporins contain channels that allow the rapid transmembrane diffusion of water but not protons.

6. Transport proteins such as GLUT1 alternate between two conformational states that expose the ligand-binding site to opposite sides of the membrane.

7. Active transport, in most cases, is driven by ATP hydrolysis. In the $(Na^+-K^+)$–ATPase and $Ca^{2+}$–ATPase, ATP hydrolysis and ion transport are coupled and vectorial.

8. In secondary active transport, an ion gradient maintained by an ATPase drives the transport of another substance. For example, the transport of lactose into a cell by lactose permease is driven by the cotransport of $H^+$.

## ◉ REFERENCES

Busch, W. and Saier, M.H., Jr., The transporter classification (TC) system, 2002, *Crit. Rev. Biochem. Mol. Biol.* **37,** 287–337 (2002). [Summarizes the classification of the nearly 400 families of transport systems and their distribution among the three domains of life.]

Dutzler, R., Schirmer, T., Karplus, M., and Fischer, S., Translocation mechanism of long sugar chains across the maltoporin membrane channel, *Structure* **10,** 1273–1284 (2002).

Kovacs, F., Quine, J., and Cross, T.A., Validation of the single-stranded channel conformation of gramicidin A by solid-state NMR, *Proc. Natl. Acad. Sci.* **96,** 7910–7915 (1999).

Unger, V.M., Kumar, N.M., Gilula, N.B., and Yeager, M., Three-dimensional structure of a recombinant gap junction membrane channel, *Science* **283,** 1176–1180 (1999).

Walmsley, A.R., Barrett, M.P., Bringaud, F., and Gould, G.W., Sugar transporters from bacteria, parasites, and mammals: structure–activity relationships, *Trends Biochem. Sci.* **22,** 476–481 (1998). [Provides structure–function analysis of sugar transporters with 12 transmembrane helices.]

### *Ion Channels*

Dutzler, R., Campbell, E.B., Cadene, M., Chait, B.T., and MacKinnon, R., X-ray structure of a ClC chloride channel at 3.0 Å reveals the molecular basis of anion selectivity, *Nature* **415,** 287–294 (2002).

Jiang, Y., Lee, A., Chen, J., Ruta, V., Cadene, M., Chait, B.T., and MacKinnon, R., X-ray structure of a voltage-dependent $K^+$ channel, *Nature* **423,** 33–41 (2003).

Yellin, G., The voltage-gated potassium channels and their relatives, *Nature* **419,** 35–42 (2002). [Reviews the mechanisms responsible for the ion selectivity, rapid transport, and gating in $K^+$ channel proteins.]

Zhou, Y., Morais-Cabral, J.H., Kaufman, A., and MacKinnon, R., Chemistry of ion coordination and hydration revealed by a $K^+$ channel–Fab complex at 2.0 Å resolution, *Nature* **414,** 43–48 (2001).

### *Aquaporins*

Agre, P. and Kozono, D., Aquaporin water channels: Molecular mechanisms for human disease, *FEBS Lett.* **555,** 72–78 (2003).

Sui, H., Han, B.-G., Lee, J.K., and Jap, B.K., Structural basis of water-specific transport through the AQP1 water channel, *Nature* **414,** 872–878 (2001).

### *Active Transporters*

Abramson, J., Smirnova, I., Kasho, V., Verner, G., Kaback, H.R., and Iwata, S., Structure and mechanism of the lactose permease of *Escherichia coli, Science* **301,** 610–615 (2003).

Hille, B., *Ionic Channels of Excitable Membranes* (3rd ed.), Sinauer Associates (2001).

Kaplan, J.H., Biochemistry of Na,K-ATPase, *Annu. Rev. Biochem.* **71,** 511–535 (2002).

Toyoshima, C. and Nomura, H., Structural changes in the calcium pump accompanying the dissociation of calcium, *Nature* **418,** 605–611 (2002); *and* Toyoshima, C., Nomura, H., and Sugita, Y., Structural basis of ion pumping by $Ca^{2+}$-ATPase of sarcoplasmic reticulum, *FEBS Lett.* **555,** 106–110 (2003).

## KEY TERMS

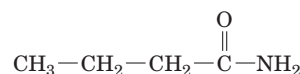| | | | |
|---|---|---|---|
| transport protein | ionophore | voltage-gated channel | antiport |
| chemical potential | carrier ionophore | depolarization | primary active transport |
| $\Delta\Psi$ | channel-forming ionophore | repolarization | secondary active transport |
| electrochemical potential | gating | action potential | gap junction |
| nonmediated transport | mechanosensitive channel | nerve impulse | pump |
| mediated transport | ligand-gated channel | uniport | permease |
| passive-mediated transport | signal-gated channel | symport | |

## STUDY EXERCISES

1. Explain why the free energy change of membrane transport depends on both the concentration and charge of the transported substance.

2. Explain the differences between mediated and nonmediated transport across membranes.

3. What are the similarities and differences among ionophores, porins, ion channels, and passive-mediated transport proteins?

4. Explain how and why ion channels are gated.

5. Use the terminology of allosteric proteins to discuss the operation of proteins that carry out uniport, symport, and antiport transport processes.

6. Distinguish passive-mediated transport, active transport, and secondary active transport.

7. Explain why the $(Na^+–K^+)$–ATPase and the $Ca^{2+}$–ATPase carry out transport in one direction only.
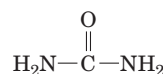
## PROBLEMS

1. Indicate whether the following compounds are likely to cross a membrane by nonmediated or mediated transport: (a) ethanol, (b) glycine, (c) cholesterol, (d) ATP.

2. Rank the rate of transmembrane diffusion of the following compounds:

$$CH_3-\overset{\overset{\displaystyle O}{\|}}{C}-NH_2 \qquad CH_3-CH_2-CH_2-\overset{\overset{\displaystyle O}{\|}}{C}-NH_2$$
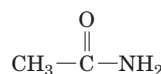
**A. Acetamide**          **B. Butyramide**

$$H_2N-\overset{\overset{\displaystyle O}{\|}}{C}-NH_2$$

**C. Urea**

3. Calculate the free energy change for glucose entry into cells when the extracellular concentration is 5 mM and the intracellular concentration is 3 mM.

4. (a) Calculate the chemical potential difference when intracellular $[Na^+]$ = 10 mM and extracellular $[Na^+]$ = 150 mM at 37°C. (b) What would the electrochemical potential be if the membrane potential were −60 mV (inside negative)?

5. For the problem in Sample Calculation 10-1, calculate $\Delta G$ at 37°C when the membrane potential is (a) −50 mV (cytosol negative) and (b) +150 mV. In which case is $Ca^{2+}$ movement in the indicated direction thermodynamically favorable?

6. (a) What happens to $K^+$ transport by valinomycin when the membrane is cooled below its transition temperature? (b) The N-terminus of gramicidin A is formylated (Fig. 10-4). Could gramicidin A form a transmembrane channel if its N-terminus were not blocked in this fashion? Explain.

7. How long would it take 100 molecules of valinomycin to transport enough $K^+$ to change the concentration inside an erythrocyte of volume 100 $\mu m^3$ by 10 mM? (Assume that the valinomycin does not also transport any $K^+$ out of the cell, which it really does, and that the valinomycin molecules inside the cell are always saturated with $K^+$.)

8. The rate of movement (flux) of a substance X into cells was measured at different concentrations of X to construct the graph below.

   (a) Does this information suggest that the movement of X into the cells is mediated by a protein transporter? Explain.

   (b) What additional experiment could you perform to verify that a transport protein is or is not involved?
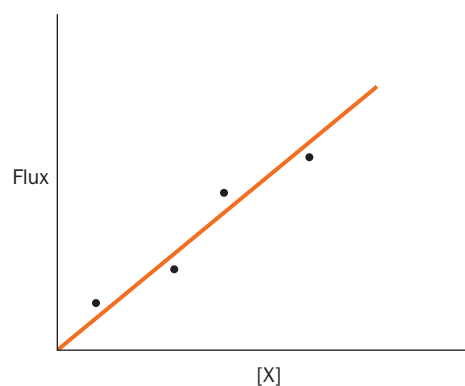


9. If the ATP supply in the cell shown in Fig. 10-24c suddenly vanished, would the intracellular glucose concentration increase, decrease, or remain the same?

10. Endothelial cells and pericytes in the retina of the eye have different mechanisms for glucose uptake. The figure shows the rate of glucose uptake for each type of cell in the presence of increasing amounts of sodium. What do these results reveal about the glucose transporter in each cell type? [Problem provided by Kathleen Cornely, Providence College.]
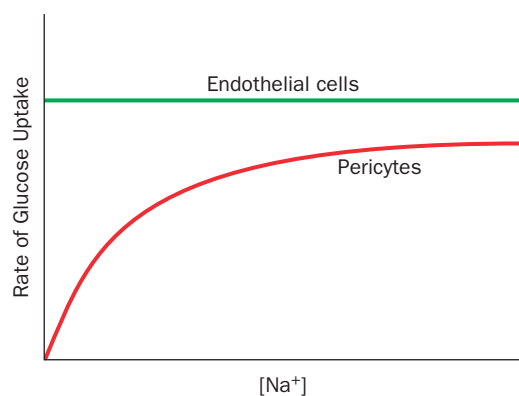


11. The compound shown below is the antiparasitic drug miltefosine.

$$CH_3-(CH_2)_{15}-O-\overset{\overset{\displaystyle O^-}{|}}{\underset{\underset{\displaystyle O}{\parallel}}{P}}-CH_2-CH_2-N^+(CH_3)_3$$
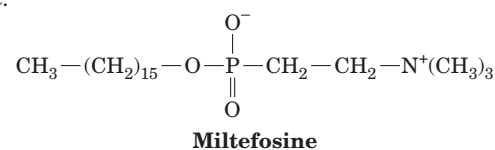
**Miltefosine**

(a) Is this compound a glycerophospholipid?

(b) How does miltefosine likely cross the parasite cell membrane?

(c) In what part of the cell would the drug tend to accumulate? Explain.

(d) Miltefosine binds to a protein that also binds some sphingolipids and some glycerophospholipids. What feature common to all these compounds is recognized by the protein? The protein does not bind triacylglycerols.

12. In eukaryotes, ribosomes (approximate mass $4 \times 10^6$ D) are assembled inside the nucleus, which is enclosed by a double membrane. Protein synthesis occurs in the cytosol. (a) Could a protein similar to a porin or the glucose transporter be responsible for transporting ribosomes into the cytoplasm? Explain. (b) Would free energy be required to move a ribosome from the nucleus to the cytoplasm? Why or why not?

13. In addition to neurons, muscle cells undergo depolarization, although smaller and slower than in the neuron, as a result of the activity of the acetylcholine receptor.

(a) The acetylcholine receptor is also a gated ion channel. What triggers the gate to open?

(b) The acetylcholine receptor/ion channel is specific for $Na^+$ ions. Would $Na^+$ ions flow in or out? Why?

(c) How would the $Na^+$ flow through the ion channel change the membrane potential?

14. Cells in the wall of the mammalian stomach secrete HCl at a concentration of 0.15 M. The secreted protons, which are derived from the intracellular hydration of $CO_2$ by carbonic anhydrase, are pumped out by an $(H^+–K^+)$–ATPase antiport. A $K^+–Cl^-$ cotransporter is also required to complete the overall transport process. (a) Calculate the pH of the secreted HCl. How does this compare to the cytosolic pH (7.4)? (b) Write the reaction catalyzed by carbonic anhydrase. (c) Draw a diagram to show how the action of both transport proteins results in the secretion of HCl.

15. Proteins known as multidrug resistance (MDR) transporters use the free energy of ATP hydrolysis to pump a variety of hydrophobic substances out of cells. (a) Write the reaction for ATP hydrolysis and explain, in structural terms, how the transporter might take advantage of this process to drive transport. There is no phosphorylated protein intermediate, as in the $(Na^+–K^+)$–ATPase. (b) Why would overexpression of an MDR transporter in a cancer cell make the cancer more difficult to treat?